Ultrafast structural phase transitions and coherent phonons in solids and nanostructures

Harald O. Jeschke

Institut für Theoretische Physik, Universität Frankfurt

X-Ray Frontiers, KITP Santa Barbara, August 31, 2010

Acknowledgments

Collaborators on bulk semiconductors and nanostructures:

Karl-Heinz Bennemann (Freie Universität Berlin)
Martin Garcia, Momar Diakhate (Universität Kassel)
Aldo Romero (CINVESTAV, Mexico)
Traian Dumitrica (University of Minnesota, USA)
Felipe Valencia (Universidad Nacional de Colombia, Bogotá).

Funding:

Emmy Noether Program of the DFG
Helmholtz Association through HA216/EMMI

Melting and ablation by an ultrashort laser pulse

An ultrashort intense laser puls hits a semiconductor target.

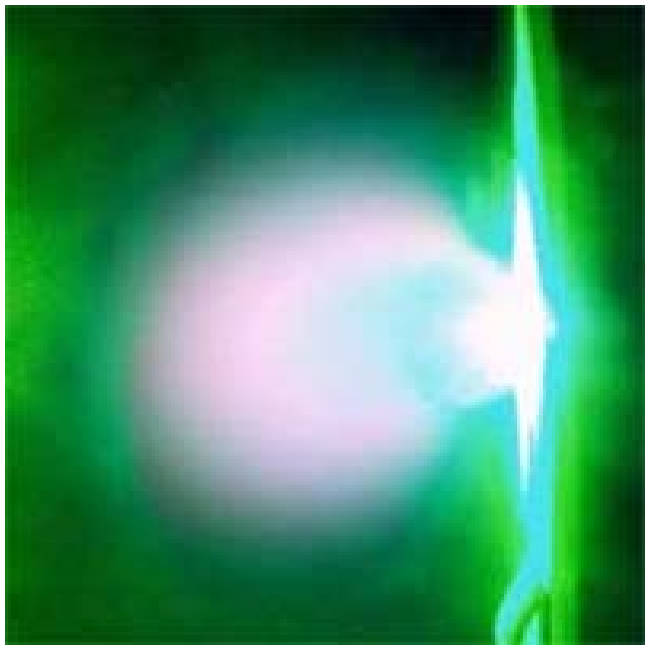

© E. Campbell, Göteborg University

Multitude of excitation and relaxation processes

$\longrightarrow$

of electrons and lattice

Oberservation of target surface with a scanning electron microscope (here InP, one and two pulses).

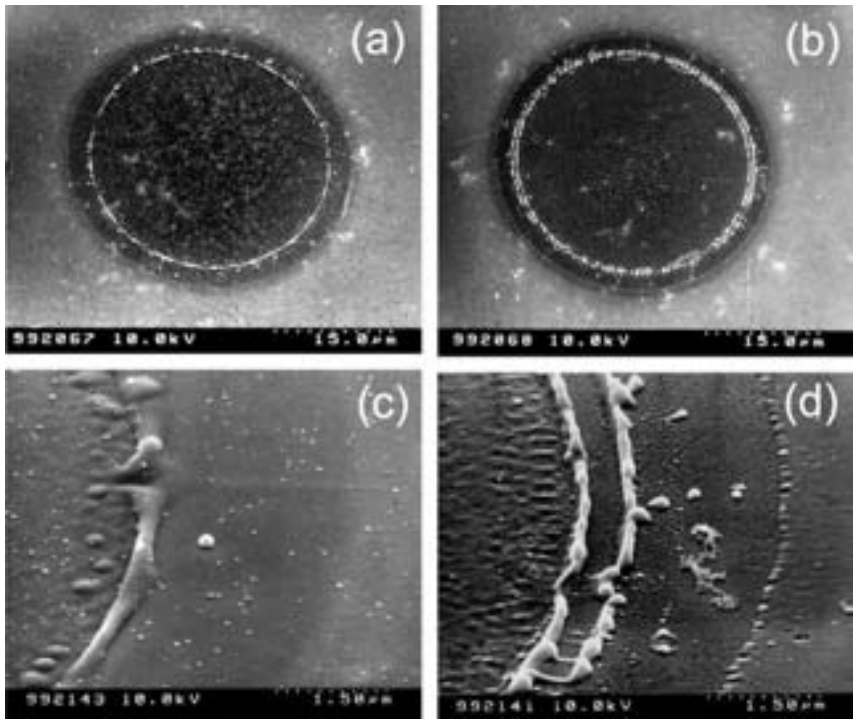

Bonse et al., App. Surf. Sci. **202**, 272 (2002)

Carbon nanostructures

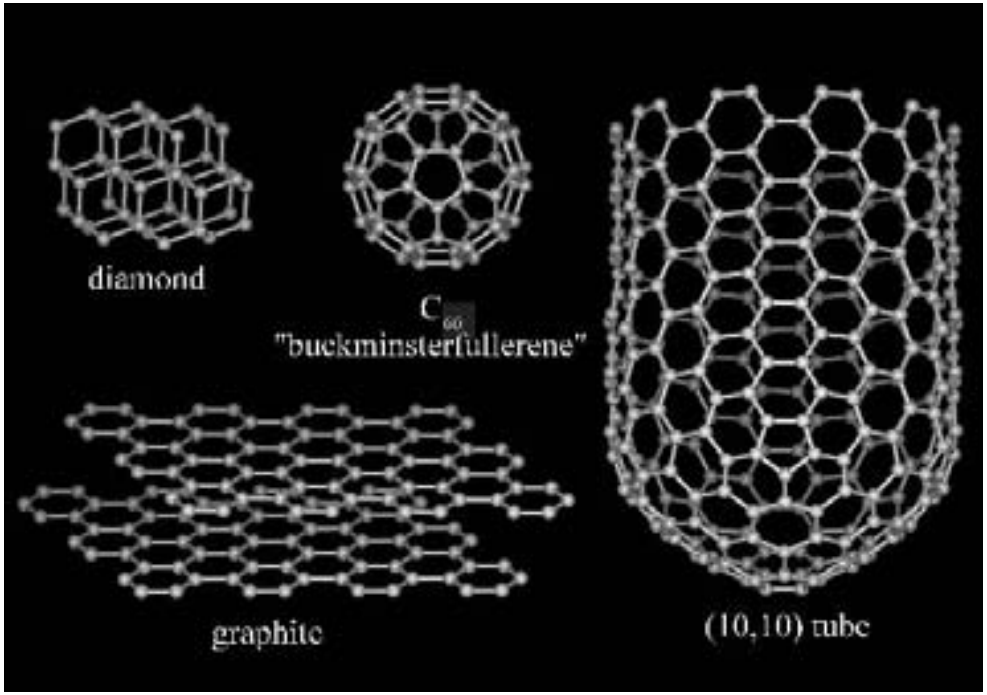

- Fully synthetic materials: Picture them as rolled up graphene sheets or as onedimensional (1D) elongated fullerenes.
- Metallic or semiconducting depending on structure.

- Realization of 1D physics.
- Unusual properties: Strongest, stiffest molecule, best molecular conductor of current and heat.
- Many open questions: Can they be produced in large quantities? Can they be grown in organized arrays or a perfect single crystal? Can they be sorted by diameter and chirality? Can they be used to make nanoelectronic devices, nanomachines?

Why study laser irradiation of carbon nanostructures theoretically?

- Carbon nanotubes can be produced in significant quantities (especially multiwall tubes).
- Grown nanotube ensembles are typically distributed over diameters and comprise many chiralities. They contain defects and even catalyst particles.
- But: Electronic properties depend crucially on geometry and perfection.

$\Rightarrow$ Efficient methods of CNT bundle manipulation are necessary! (Tips of scanning force microscopes are not enough).

Due to finely tunable parameters, a pulsed laser is a promising tool.

$\triangleright$ Theory can explore the possibilities!

Macroscopic versus microscopic description

Macroscopic:

Hydrodynamics

Differential equations for density, momentum and energy of a material.

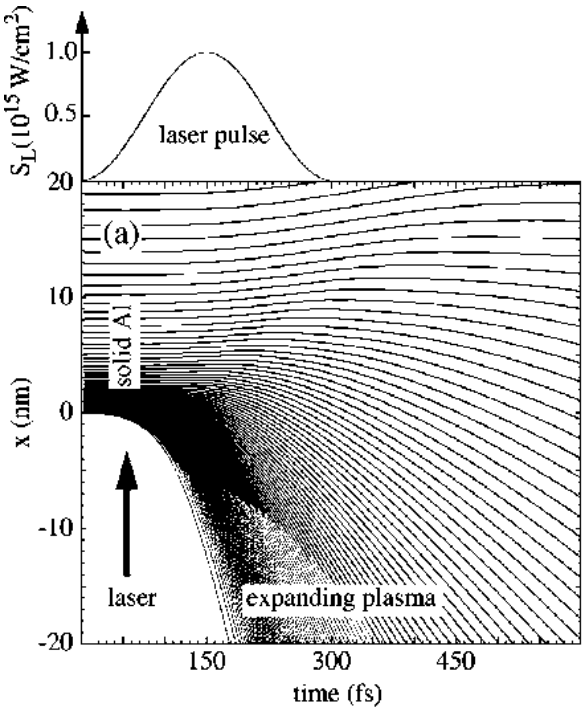

Eidmann et al., Phys. Rev. E **62**, 1202 (2000)

Microscopic:

Mechanik

Equations of motion for the atoms of a material: **Molecular dynamics**.

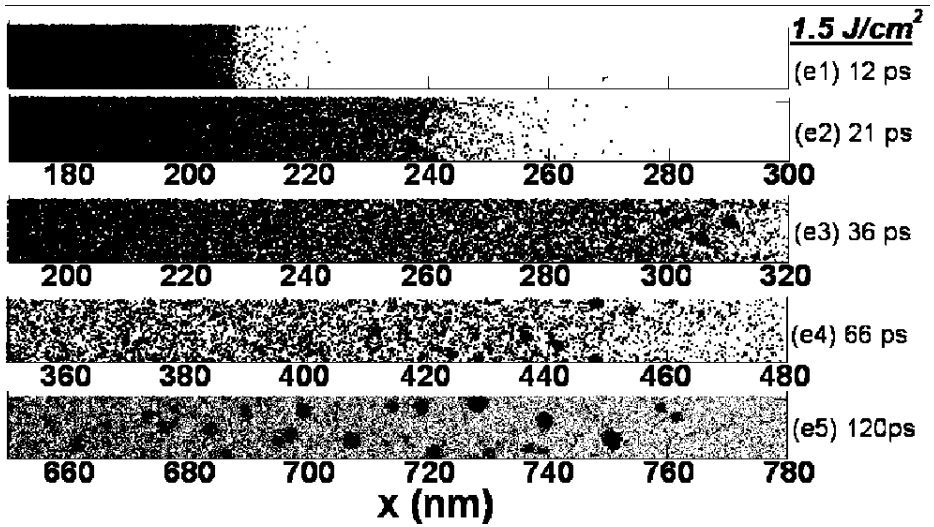

Cheng, Xu, Phys. Rev. B **72**, 165415 (2005)

$\longrightarrow$ Interactions between the atoms can be treated at different levels of accuracy.

Choice of interaction potential

Force field methods

- Parametrized potentials for the interaction between 2, 3 or more atoms.
- Can treat millions of atoms.
- Knows nothing of electrons (chemistry, laser excitation).

Tight binding molecular dynamics

- Parametrization of overlap integral of atomic wave functions.
- Can treat one thousand atoms.
- Chemistry described decently, laser with additional equations.

Ab initio molecular dynamics

- Quantum mechanical description.
- Can treat two hundred atoms.
- Chemistry described very well, laser not so simple.

Modelling geometry

a) Molecular dynamics (MD) at constant pressure

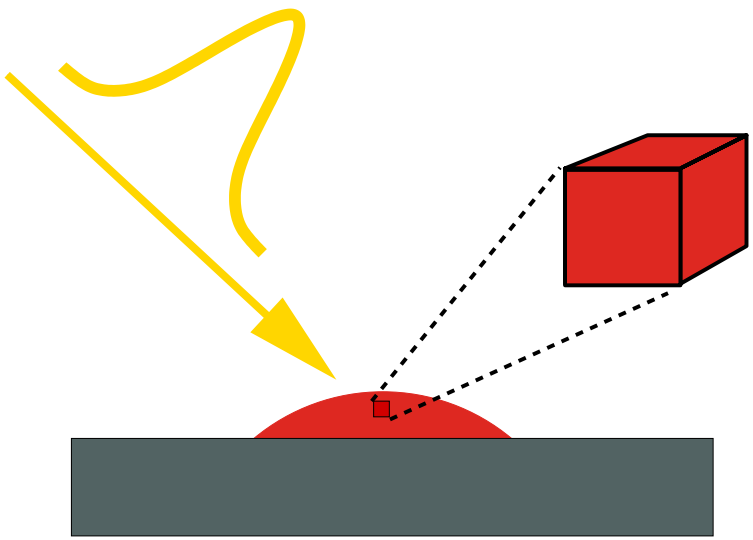

MD unit cell with periodic boundary conditions rapidly changes shape and volume.

b) Molecular dynamics for a film geometry

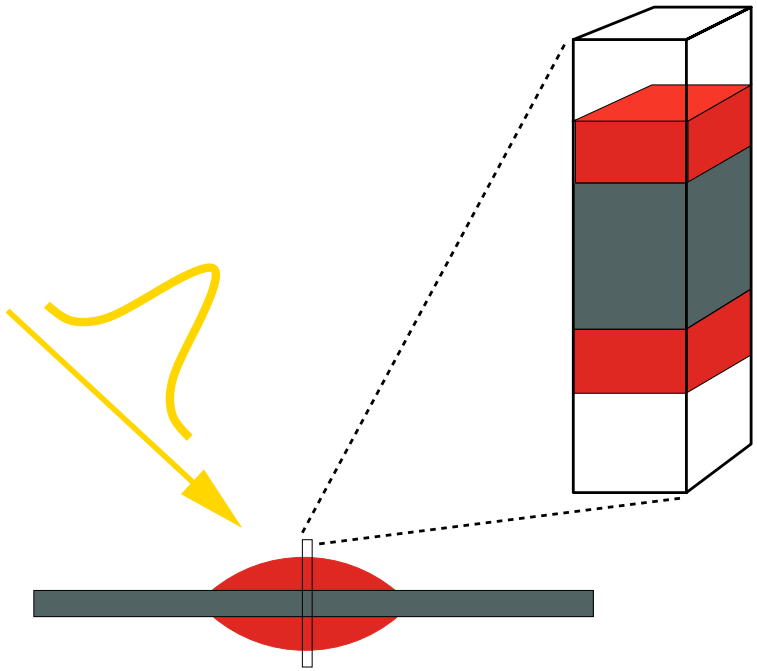

Fixed periodic boundary conditions in x and y directions, vacuum above and below the film.

Physical picture

Electronic occupations determine interatomic interactions:

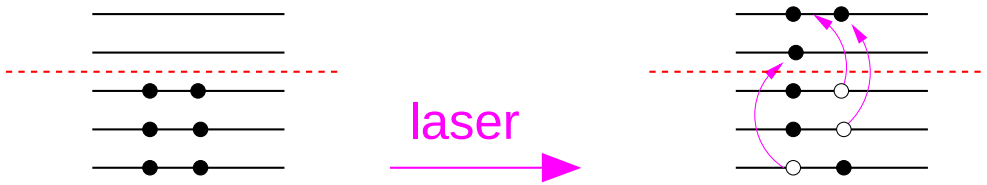

ground state
(cold electrons)

excited state
(hot electrons and holes)

no forces

interatomic forces

Size and distance dependence of interaction potential $U(\{r_{ij}\}, t)$ is changed by ultrafast excitation.

Tight binding molecular dynamics

Molecular dynamics (MD) based on Lagrange function (Andersen 1980, Parrinello, Rahman 1980)

$$L(t) = \sum_{i=1}^{N} \frac{m_i}{2} \dot{\mathbf{s}}_i^{\mathrm{T}} h^{\mathrm{T}} h \dot{\mathbf{s}}_i + K_{cell} - U(\{r_{ij}\}, t) - P\Omega \,,$$

$\mathbf{s}_i \equiv$ relative coordinates; MD unit cell spanned by **a**, **b** and **c**, (3×3) matrix $h = (\mathbf{a}\ \mathbf{b}\ \mathbf{c}) \Rightarrow \mathbf{r}_i = h\mathbf{s}_i$, $r_{ij} = |\mathbf{r}_i - \mathbf{r}_j|$.
$K_{cell} \equiv$ kinetic energy of MD unit cell,
$U(\{r_{ij}\}, t) \equiv$ interaction potential.

$\Rightarrow$ **Equations of motion** for coordinates $\mathbf{s}_i$ and unit cell h_{kl}.

Interatomic interaction potential

$$U(\{r_{ij}\}, t) = \sum_m n(\epsilon_m, t)\, \epsilon_m + \Phi_{rep}(\{r_{ij}\}) \,,$$

$\Phi_{rep} \equiv$ ion ion repulsion; $\epsilon_m = \langle m | H_{\mathrm{TB}} | m \rangle \equiv$ eigenvalues of the tight binding Hamiltonian $H_{\mathrm{TB}} = \sum_{i\alpha} \epsilon_{i\alpha} n_{i\alpha} + \sum_{\substack{ij\alpha\beta \\ j \neq i}} t_{ij}^{\alpha\beta} c_{i\alpha}^{+} c_{j\beta}$,

Beyond tight binding molecular dynamics

$n(\epsilon_m, t) \equiv$ occupation of electronic energy levels
(dependence on time is nonstandard!).

$\Rightarrow$ **Forces:** $\mathbf{F}_i = -\frac{\partial U(\{r_{ij}\},t)}{\partial \mathbf{s}_i}$ and $\mathbf{F}_{\alpha\beta} = -\frac{\partial U(\{r_{ij}\},t)}{\partial h_{\alpha\beta}}$ (unit cell deformation; in nanotubes: longitudinal expansion and contraction).

Electron dynamics in nonequilibrium:

$$\frac{dn(\epsilon_m,t)}{dt} = \int_{-\infty}^{\infty} d\omega\, g(\omega,t)\Big\{ n(\epsilon_m - \hbar\omega, t) + n(\epsilon_m + \hbar\omega, t) - 2n(\epsilon_m, t)\Big\} - \frac{n(\epsilon_m,t) - n^0(\epsilon_m, T_{el})}{\tau_1}$$

$g(\omega, t) \equiv$ spectral distribution of laser pulse (pulse envelope, color).
$\epsilon_m \longrightarrow \epsilon_m \pm \hbar\omega$. $\tau_1 \equiv$ thermalization time of electrons

In equilibrium: $n = n^0(\epsilon_m, T_{el}) = \left[\exp\{\frac{\epsilon_m - \mu}{k_B T_{el}}\} + 1\right]^{-1}$ Fermi function, with electron temperature $T_{el}(t)$.

Ultrafast laser induced graphitization of diamond

- Laser pulse $\tau = 20$ fs duration, $E_0 = 0.9$ eV/atom, $p = 1$ GPa.

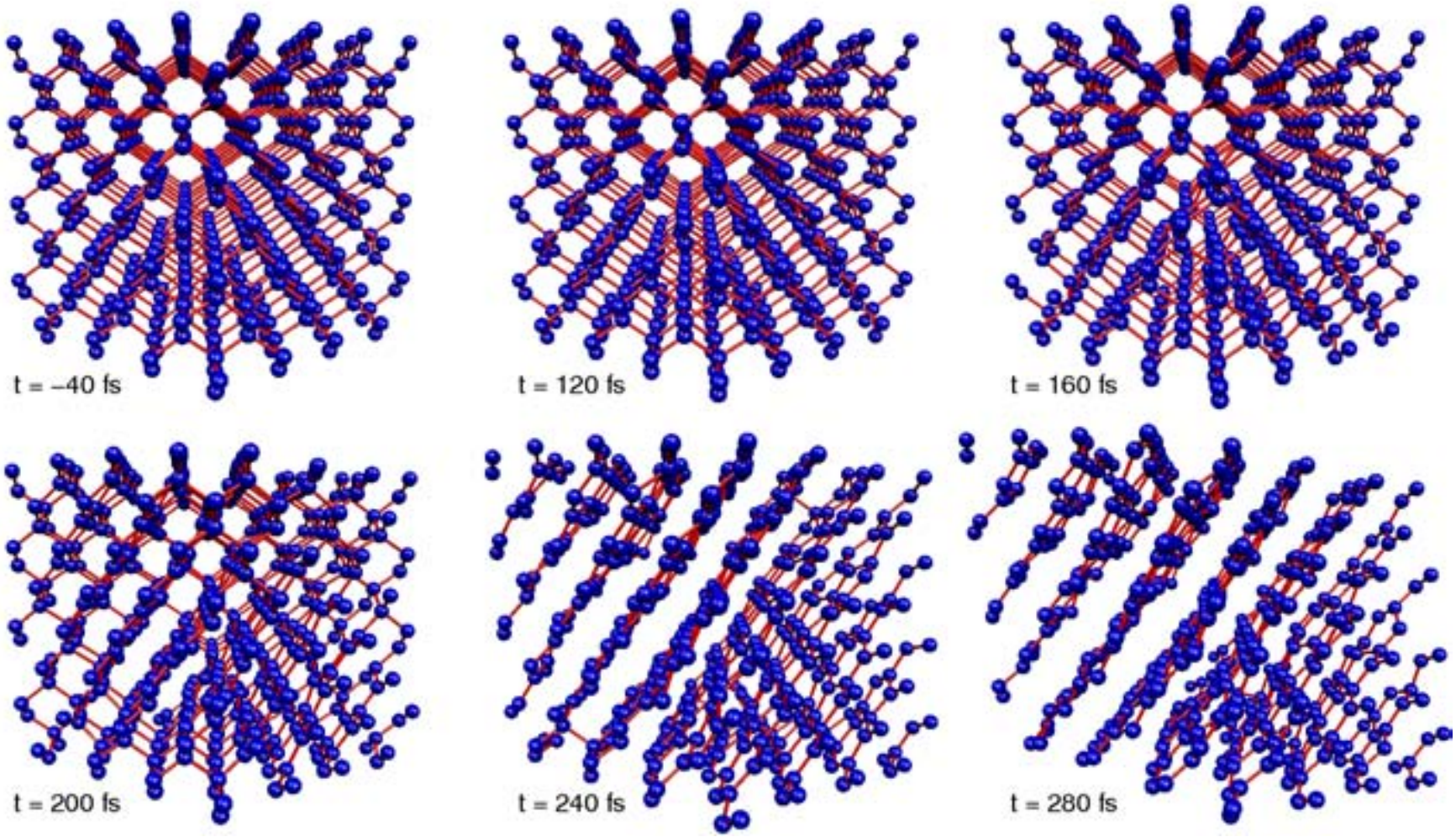

Jeschke, Garcia, Bennemann, Phys. Rev. B **60**, R3701 (1999).

X-ray diffraction spectra during laser induced graphitization of diamond

- Kinematic scattering theory
- Scattering intensity I simulated as scattering amplitude of all atoms
  $I \sim \left| \sum_j f_j^{(0)} E_e e^{2\pi i \mathbf{r}_j (\mathbf{k}-\mathbf{k}')} \right|^2$
- Diamond, $\tau = 20$ fs pulse, $E_0 = 0.9$ eV/atom, Graphitization at time $t \approx 200$ fs.
  Pietrzyk, Jeschke, Garcia, unpublished.

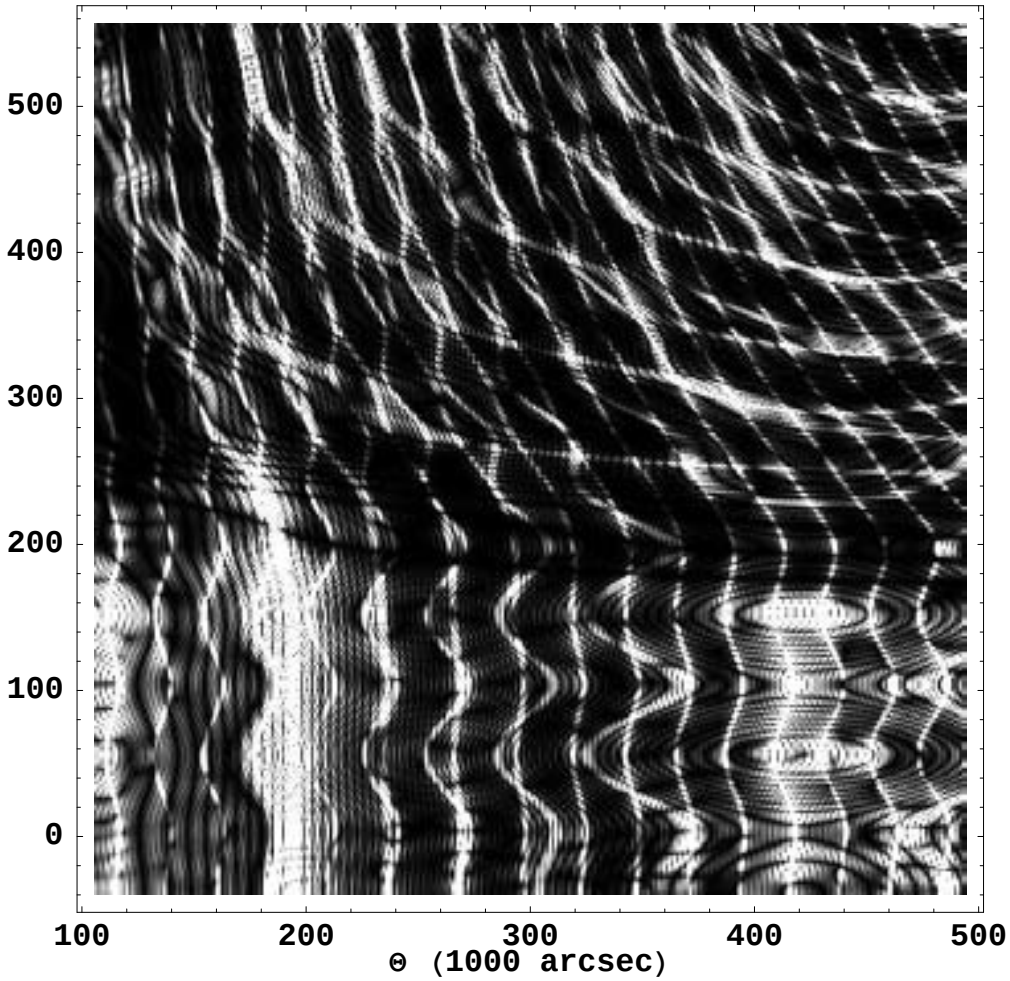

High intensity: Melting of graphite

$t = 0$ fs

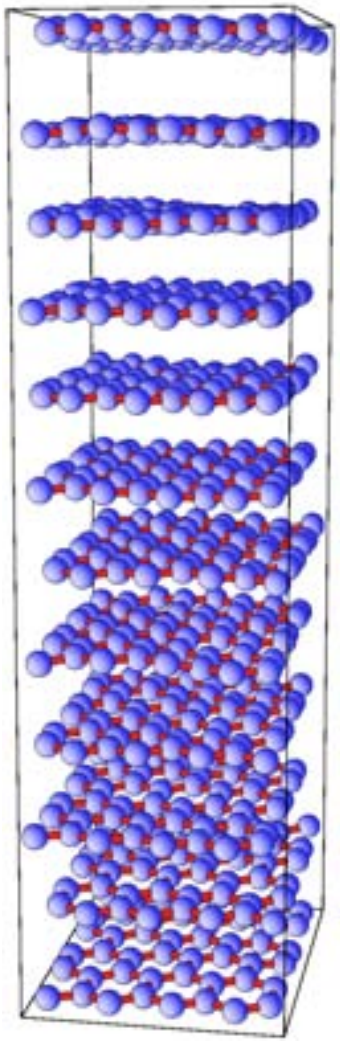

$t = 40$ fs

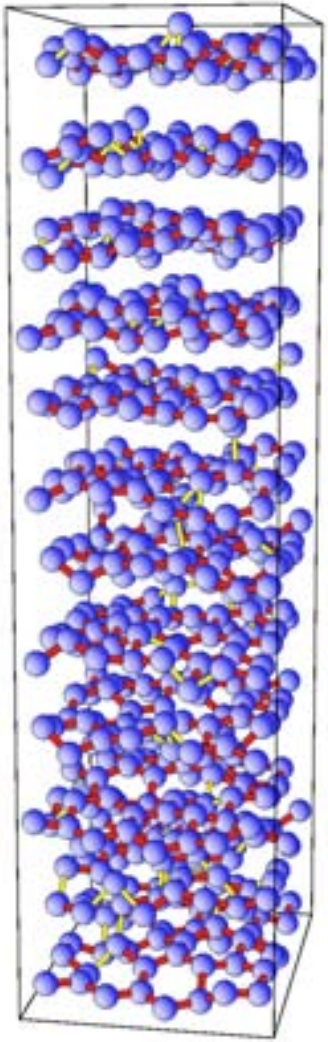

$t = 80$ fs

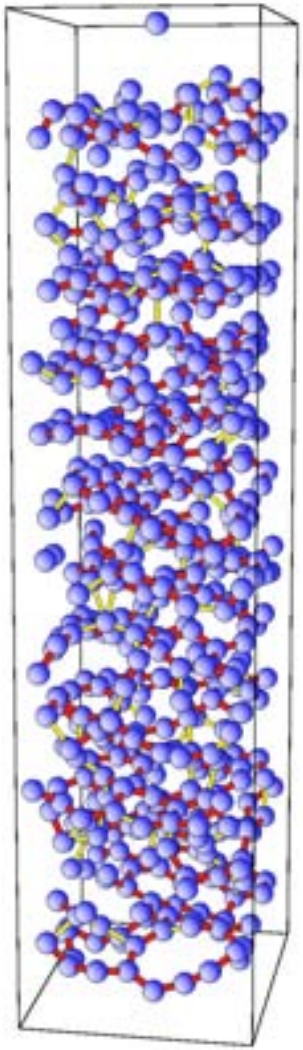

$t = 140$ fs

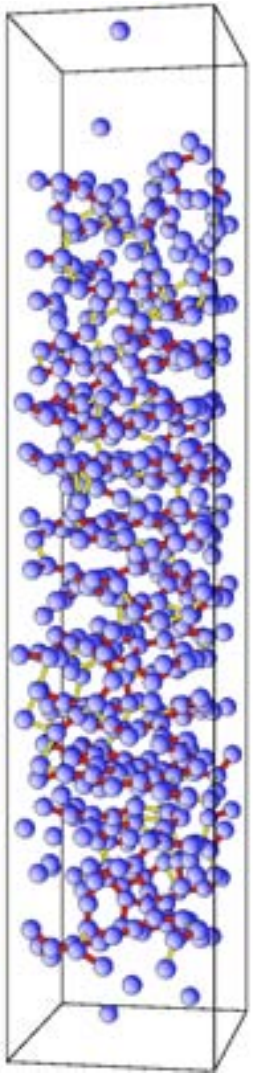

High intensity: Ablation of graphite

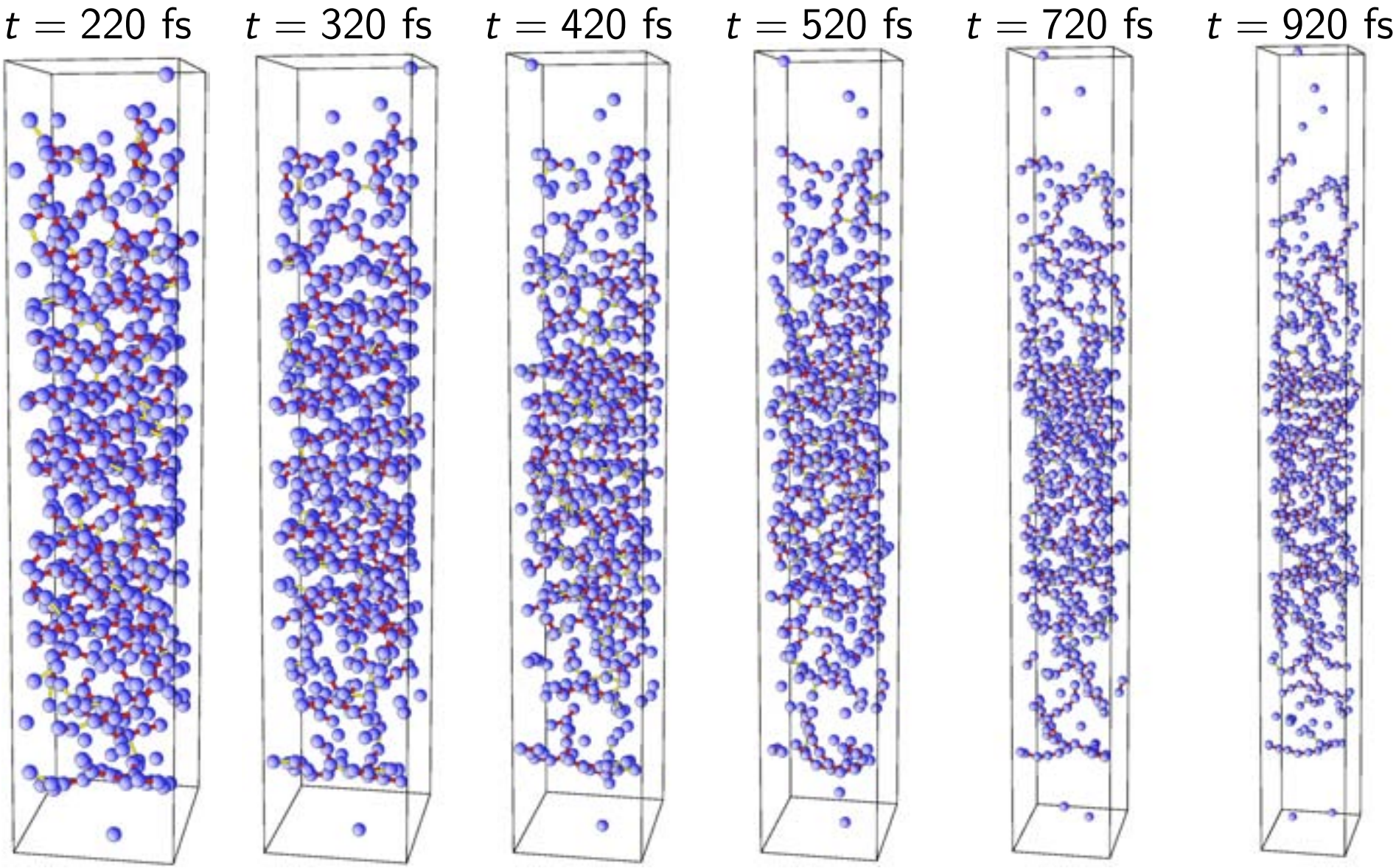

Moderate intensity: New graphite ablation mechanism

$t = 0$ fs $t = 80$ fs $t = 160$ fs $t = 860$ fs

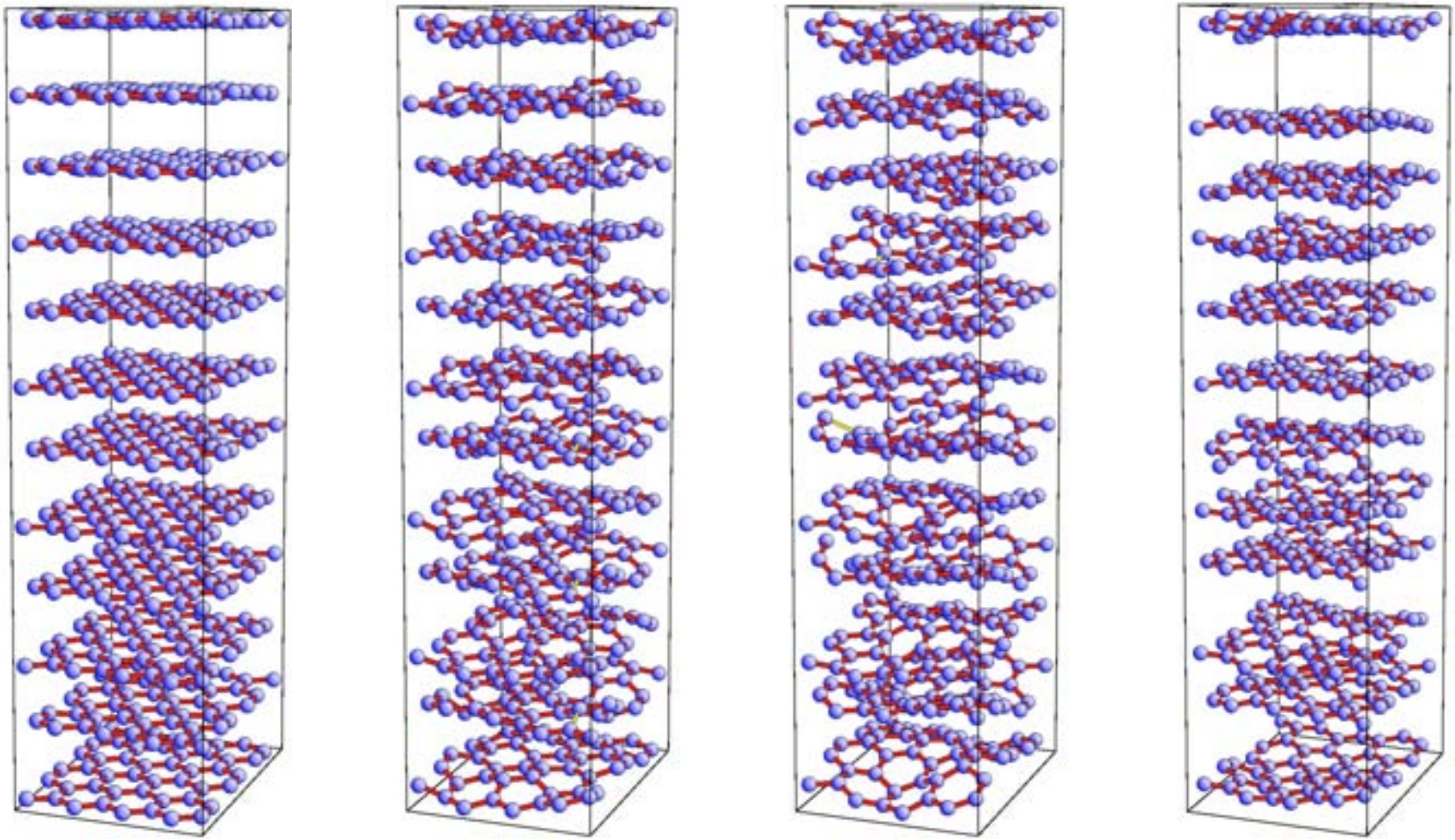

Jeschke, Garcia, Bennemann, Phys. Rev. Lett. **87**, 015003 (2001).

Experimental observation of new ablation mechanism

- Carbone, Baum, Rudolf, Zewail, Phys. Rev. Lett. **100**, 035501 (2008).
- Time resolved diffraction spectra from electron crystallography.
- Excitation below damage threshold of 130 mJ/cm^2.

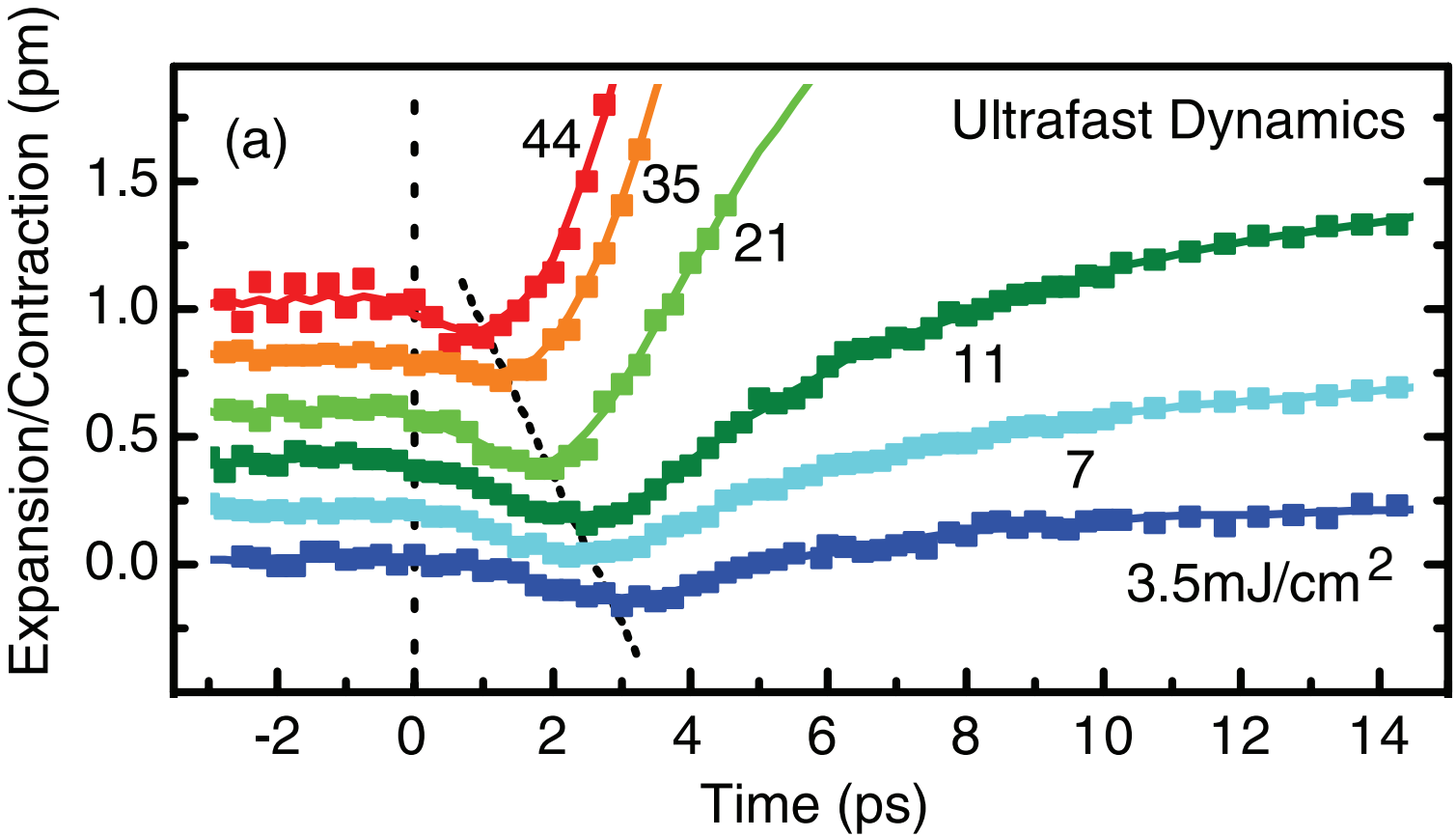

High intensity: Silicon film melting and ablation

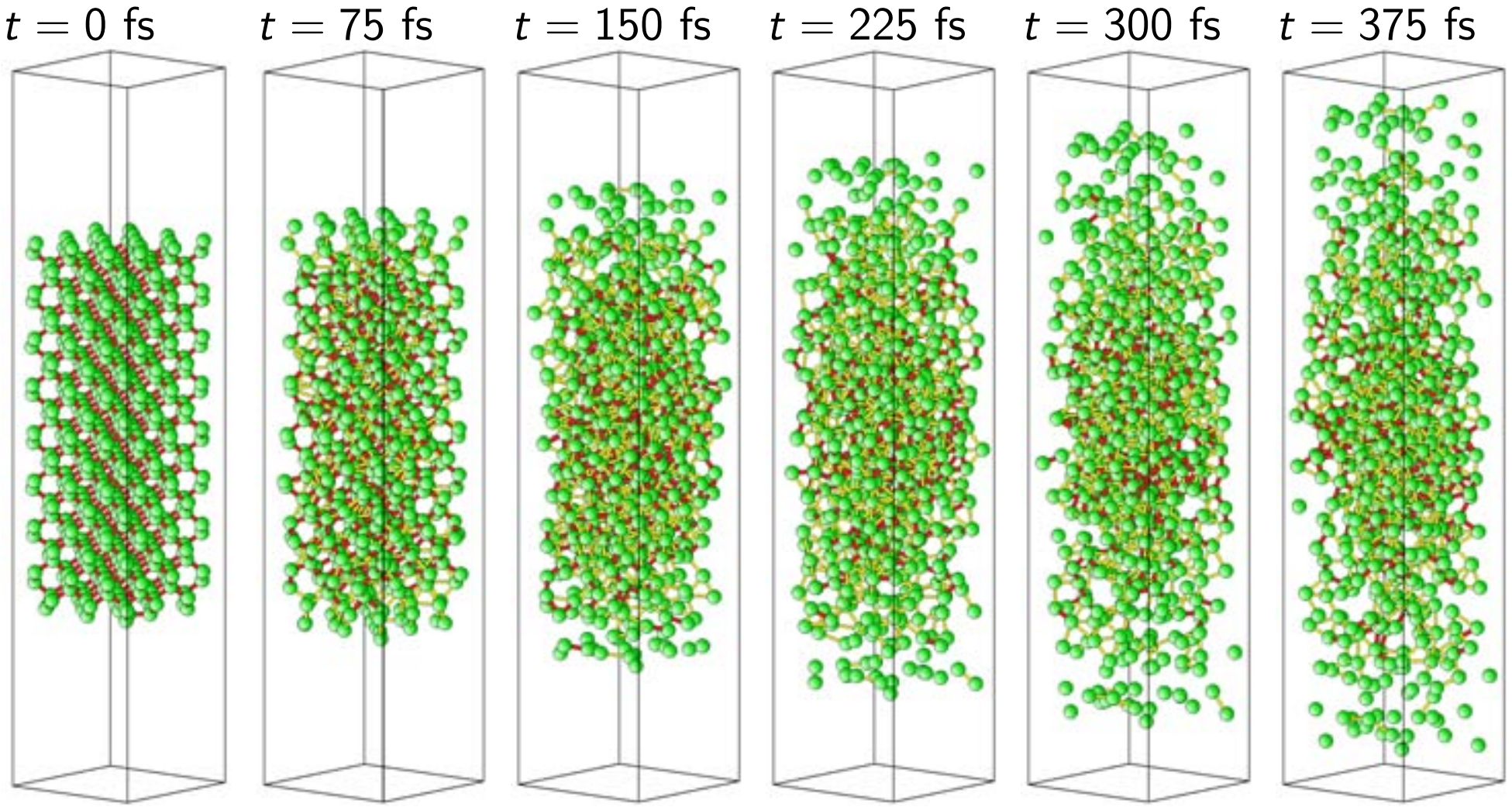

$\tau = 20$ fs pulse, $E_0 = 6.1$ eV/atom: ultrafast melting, ablation

Moderate Intensity: Large silicon cluster formoration

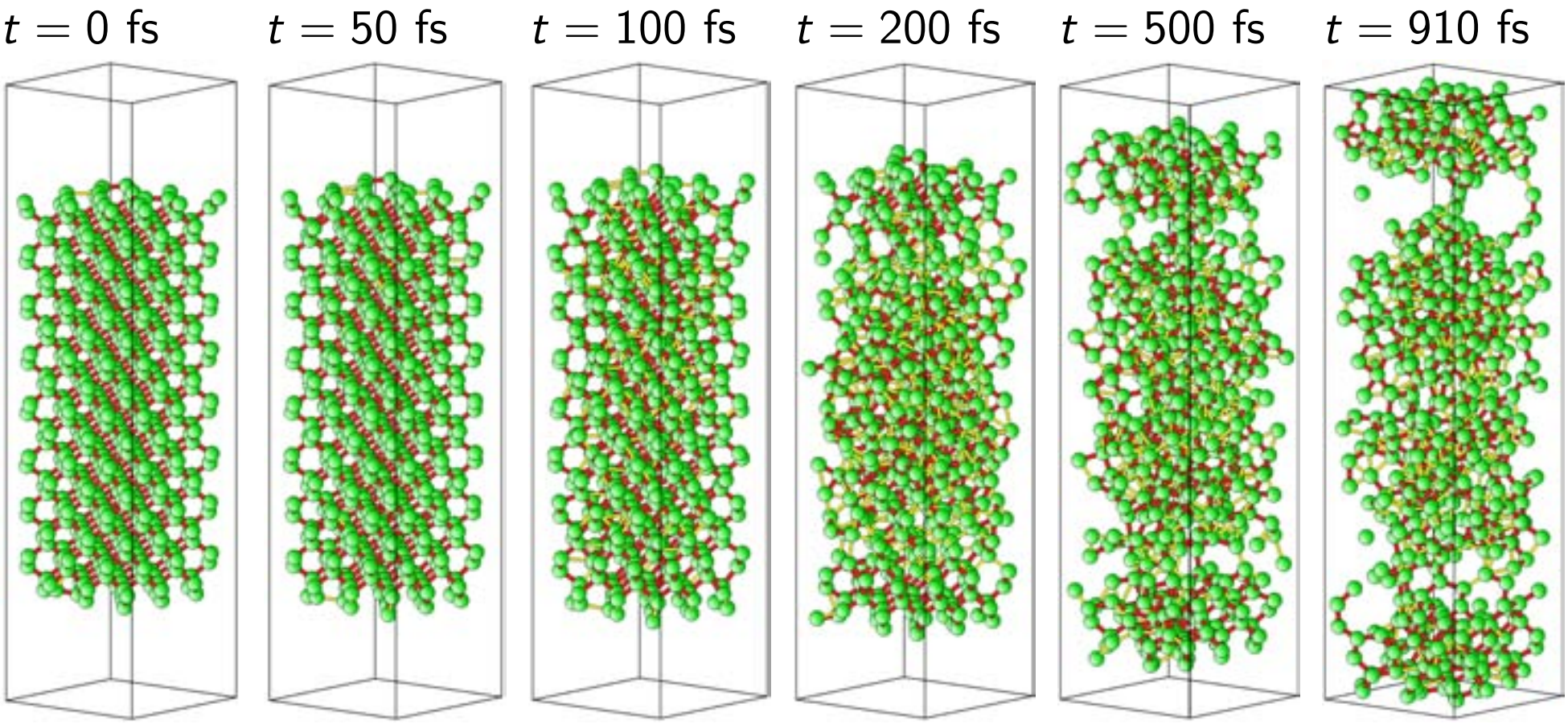

$\tau = 5$ fs pulse, $E_0 = 3.5$ eV/atom: density modulations, ablation of thick Si slabs, compare Glover *et al.*, Phys. Rev. Lett. **90**, 236102 (2003).
Jeschke, Garcia, in preparation.

Destruction of CNT at high energies

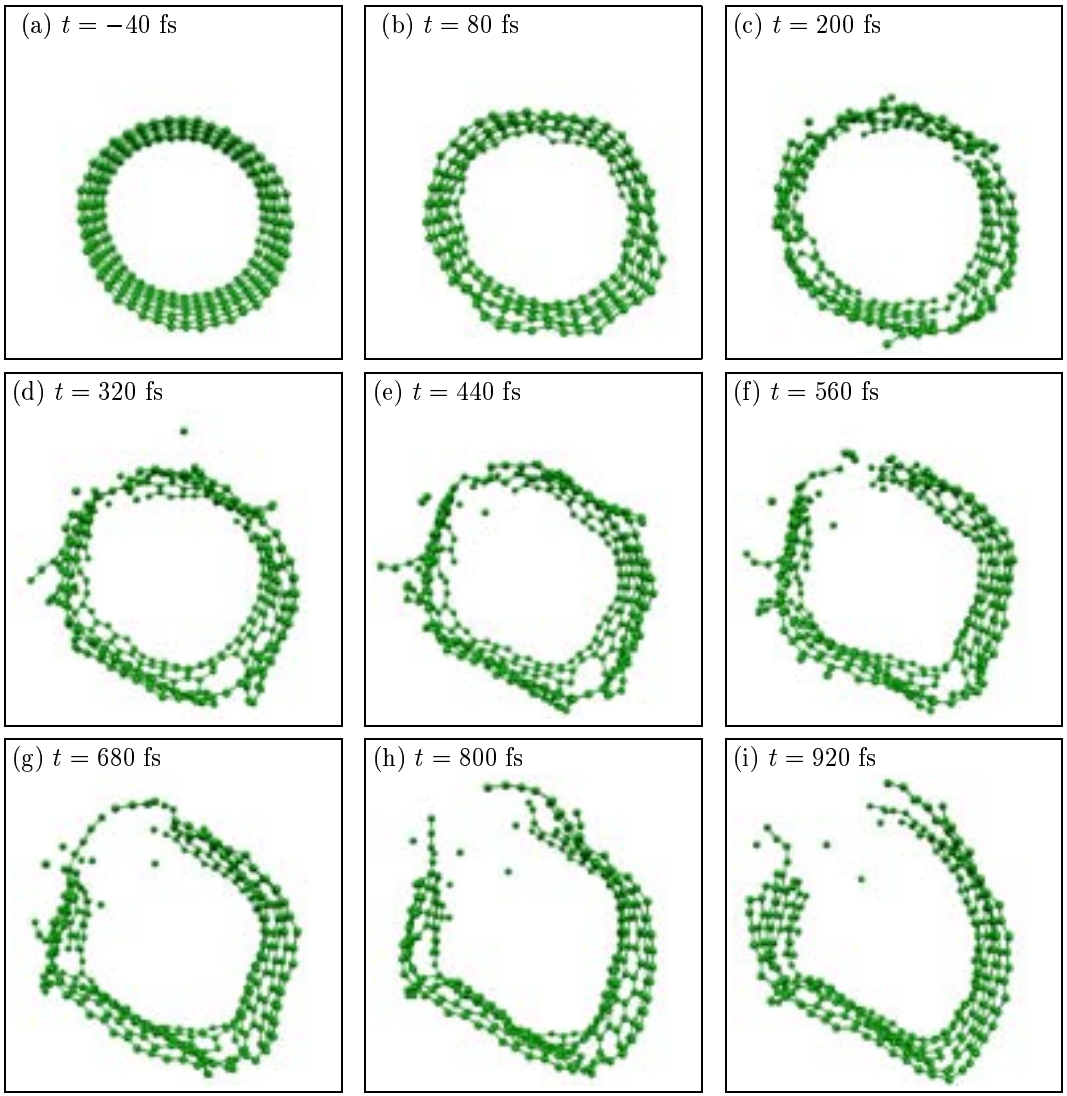

- View along a (22,0) single wall nanotube.
- Periodic boundary conditions make this tube infinite in length.
- Laser pulse of $\tau = 20$ fs duration acts at time $t = 0$.
- Laser intensity 30% above damage threshold.
- Energy suffices for **massive bond breaking** and destruction of CNT wall.

CNT damage slightly above threshold

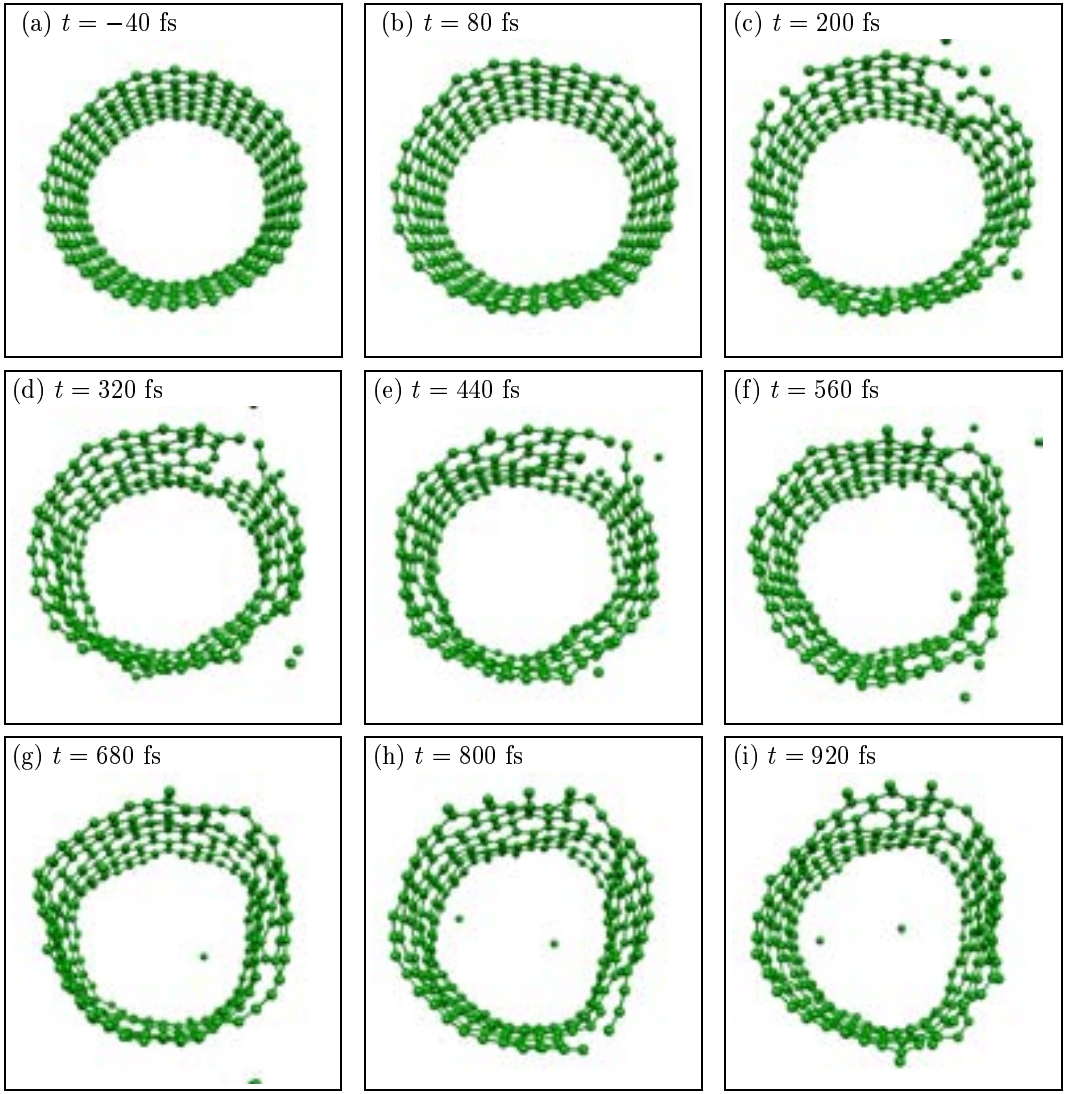

- View along a (20,0) single wall nanotube.
- Laser pulse of $\tau = 20$ fs duration with an intensity of only 8% above the damage threshold.
- CNT is damaged by emission of carbon atoms or small clusters.

Strong vibrational excitation slightly below threshold

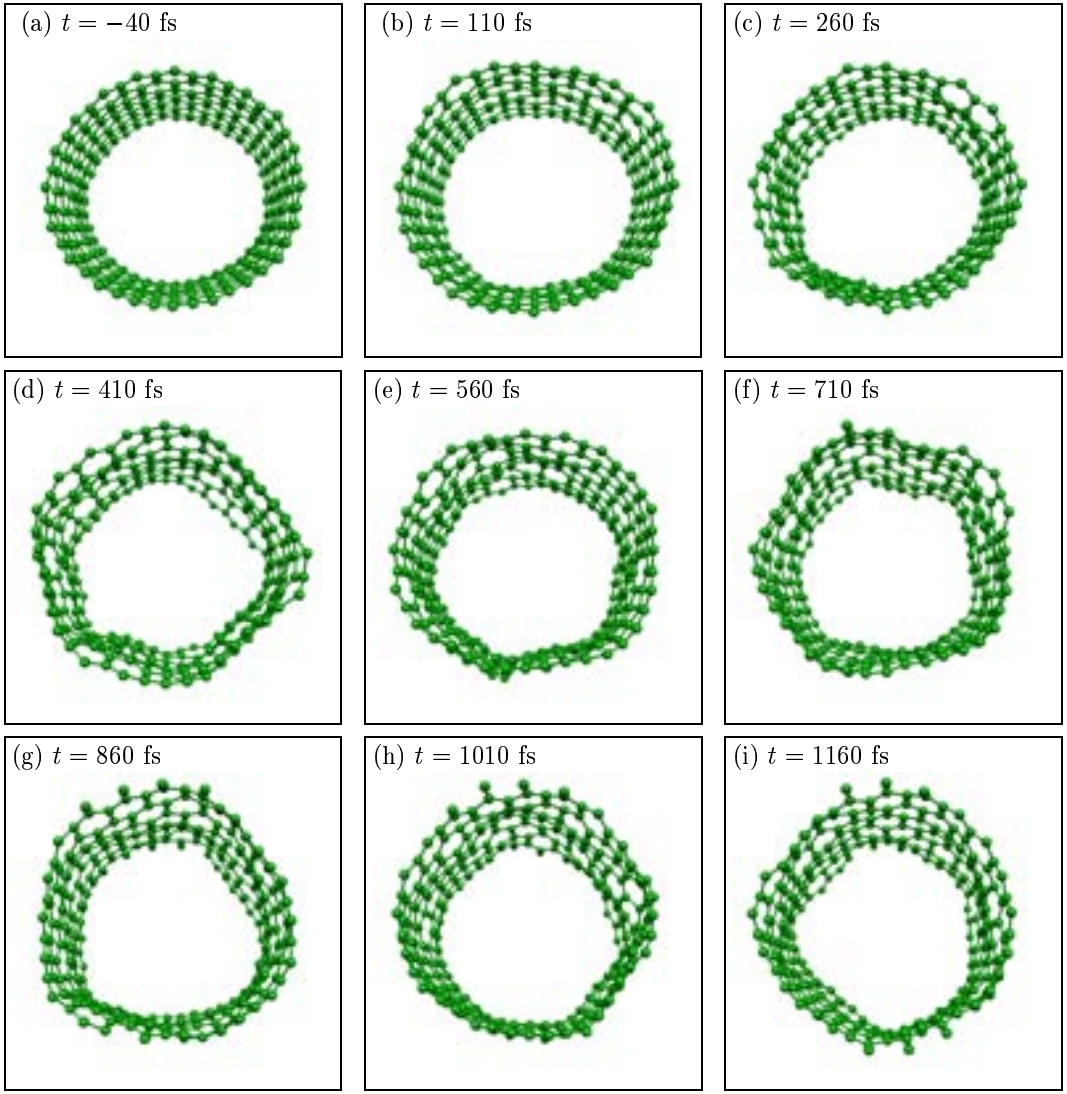

- View along a (20,0) single wall nanotube.
- Laser pulse of $\tau = 20$ fs duration with an intensity 4% below the damage threshold.
- SWNT wall stays intact (no bond breaking) but shows strong oscillations.
- ▷ What is the nature of these vibrations?

Analysis of SWNT vibrational excitation

Plan: cut up $(22, 0)$ CNT into eight 44 atom sections, fit coordinates to nearest circle by minimizing the function $f(x_0, y_0, r) = \sum_{i=1}^{N_{\text{slab}}} \left(\sqrt{(x_i - x_0)^2 + (y_i - y_0)^2} - r \right)^2$

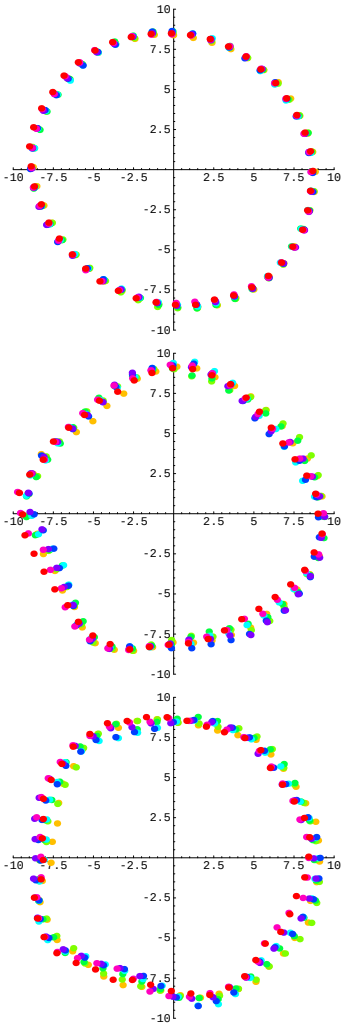

Projected slabs: Time

$t = 0$ ps

$t = 0.9$ ps

$t = 1.9$ ps

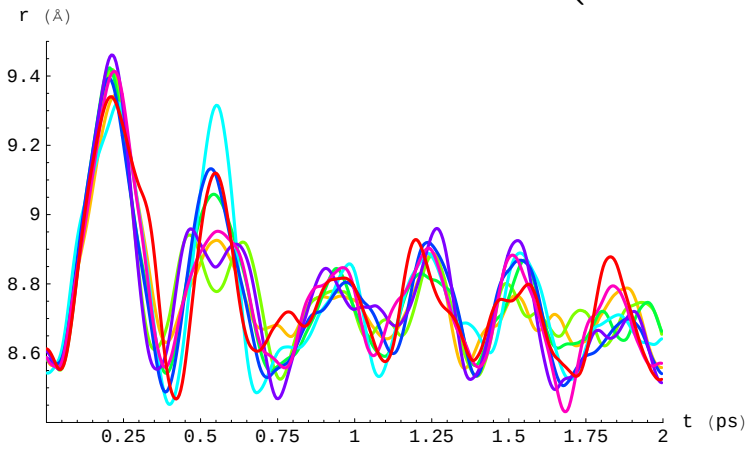

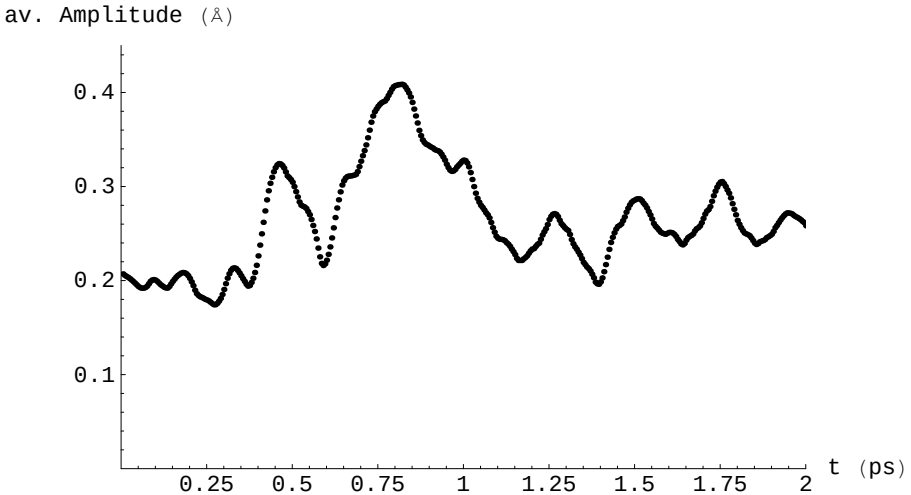

Zigzag SWNT damage thresholds as a function of diameter

Thresholds for pulse duration $\tau = 20$ fs, frequency $\hbar\omega = 1.96$ eV, given in absorbed energy E_0 per atom, extracted from many trajectories:

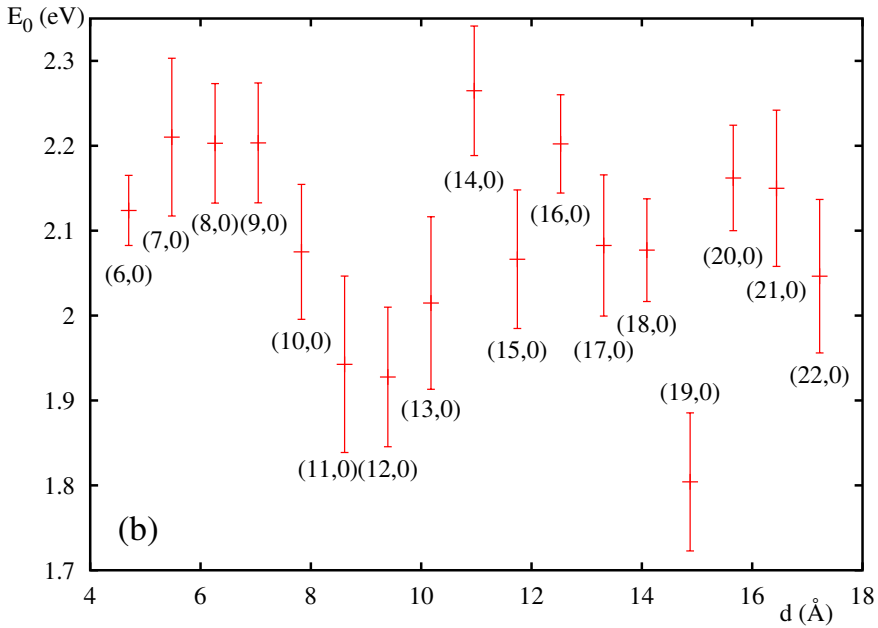

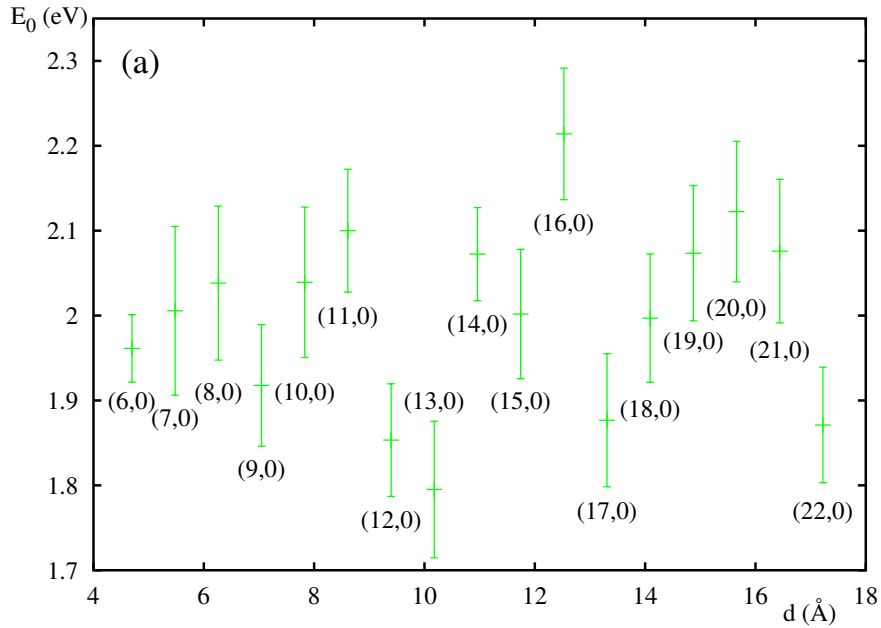

- *Bondary conditions allow longitudinal expansion*

- *Bondary conditions suppress longitudinal expansion*

- Possibility of longitudinal expansion leads to higher stability
- **Nonmonotonous diameter dependence of stability**

Armchair SWNT damage thresholds

Diameter and boundary condition dependence

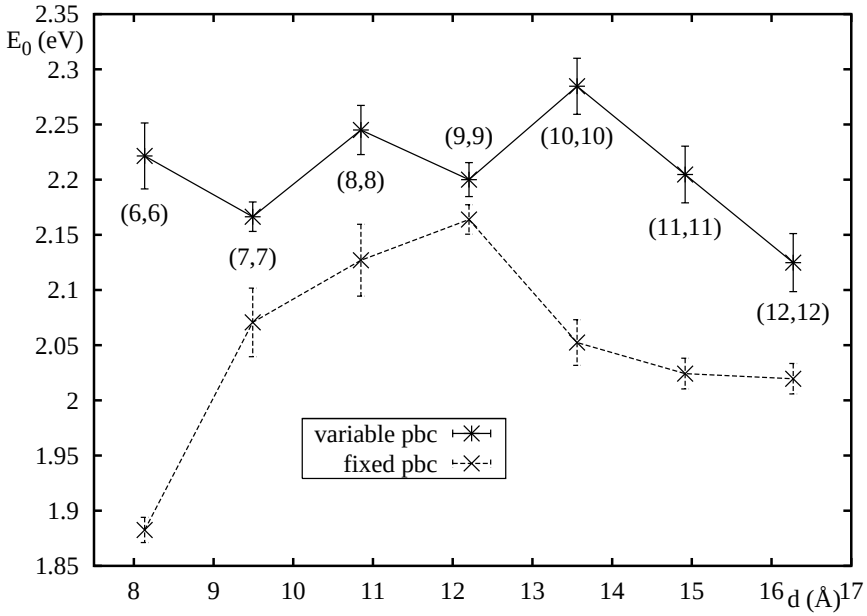

- Similarities to zigzag CNTs:
  - Stability maximum at $d \approx 12$ Å
  - Longitudinal expansion increases stability

Diameter and pulse duration dependence

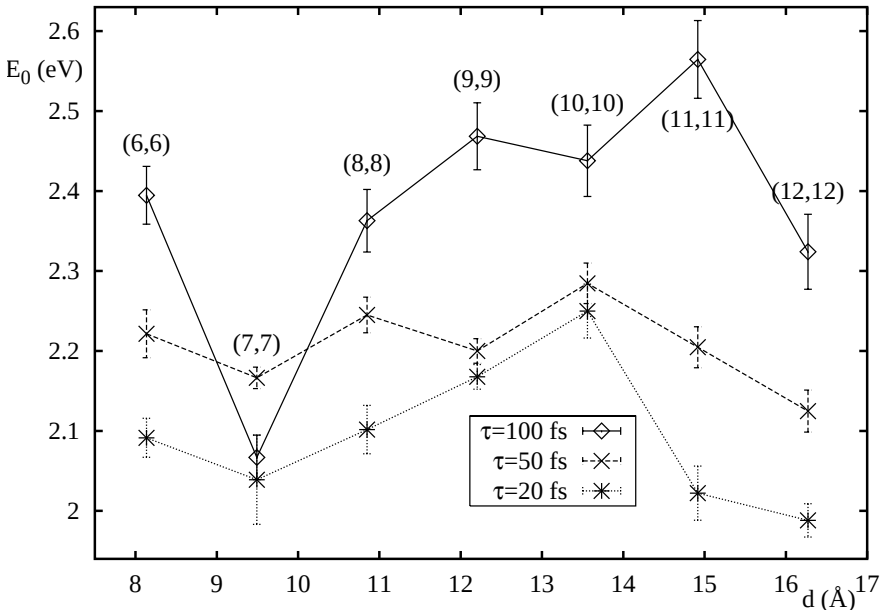

- Stability increases with pulse duration! Energy has more time to distribute over degrees of freedom during longer pulse.

Jeschke, Romero, Garcia, Rubio, Phys. Rev. B **75**, 125412 (2007).

Stone-Wales defect in graphite: Minimum energy path

- Pentgon-heptagon (Stone-Wales) defect in a graphene sheet: one carbon dimer rotated by 90° with respect to regular position.
- Climbing image nudged elastic band (CI-NEB) method based on DFT description yields minimum energy path for defect elimination.

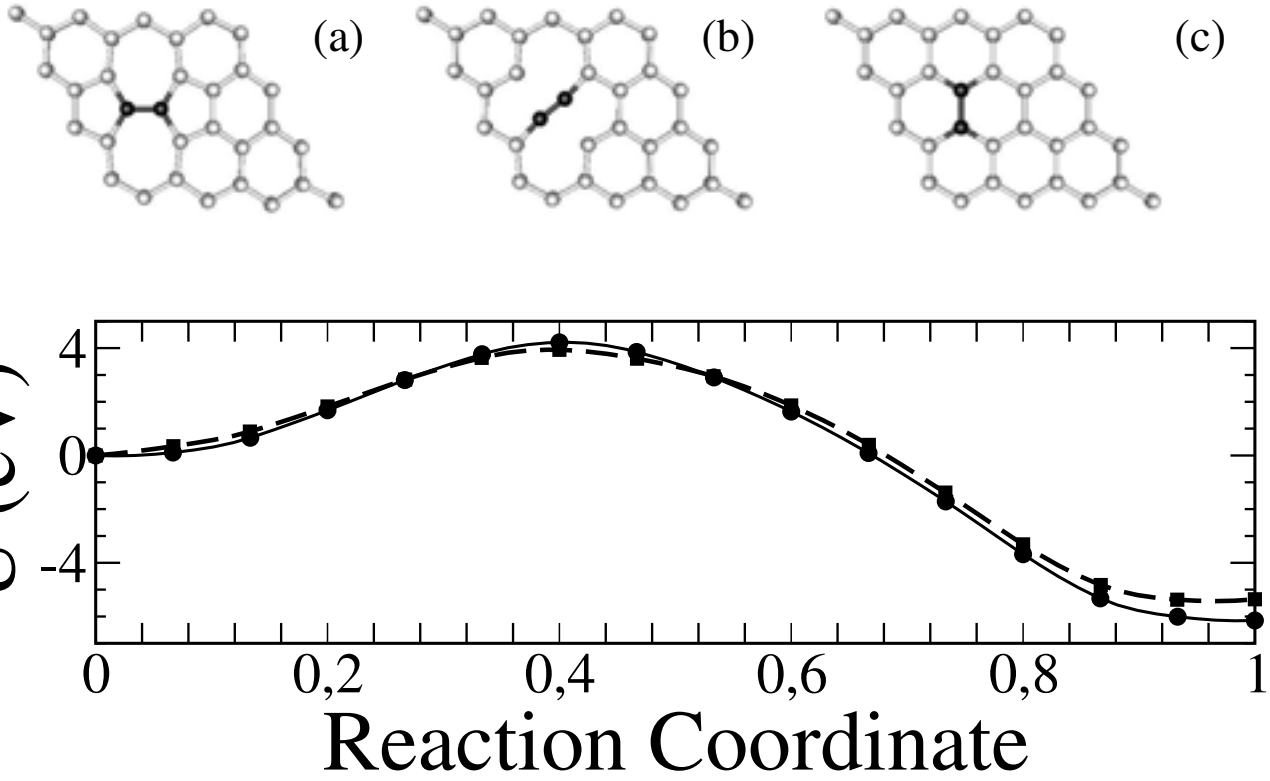

- Barrier of $E_b \approx 4$ eV means high thermal stability of defect.
- Barrier well reproduced with TB (dashed).

Stone-Wales defect in graphite: Laser healing

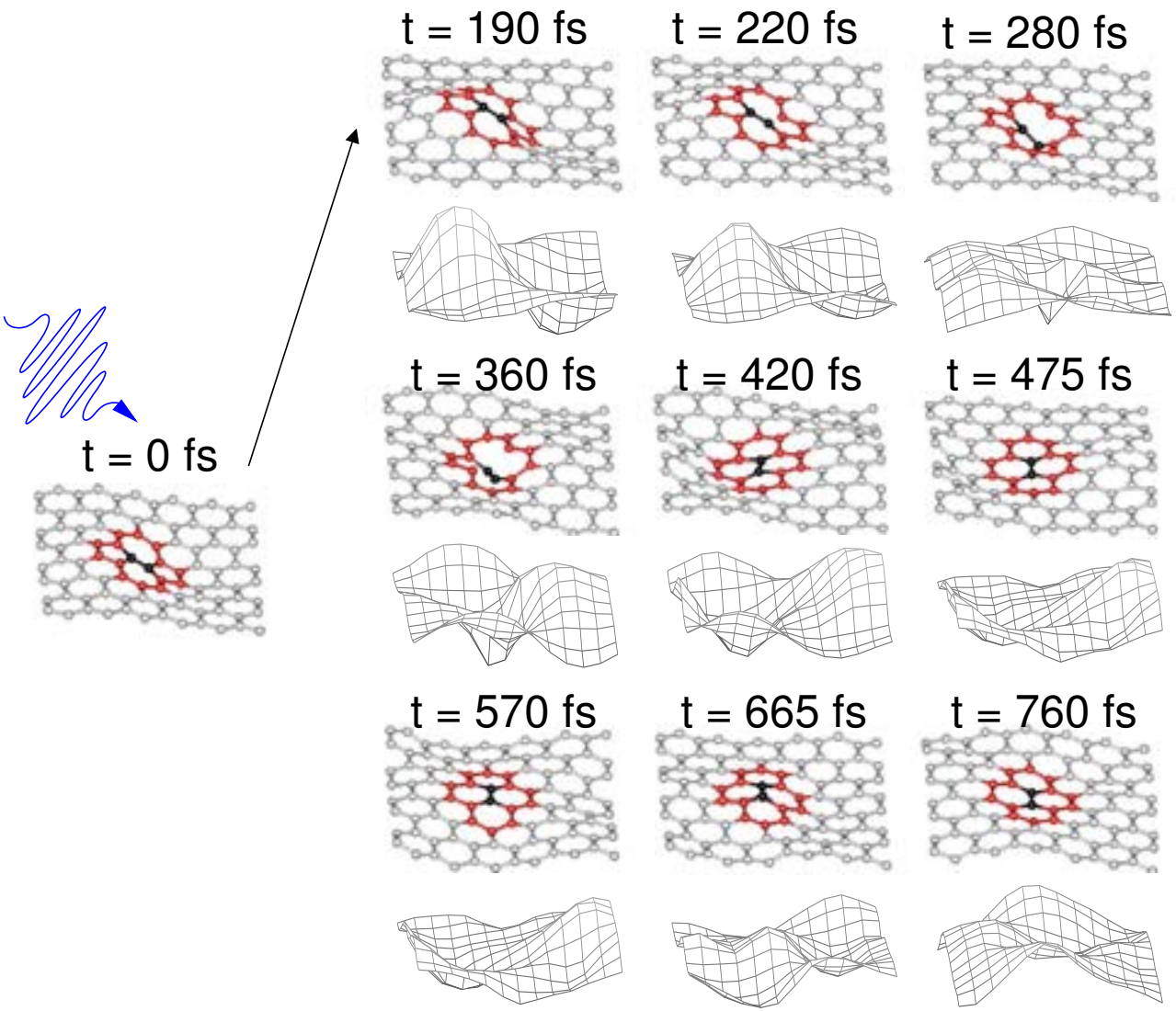

- Laser excitation of 6% of valence electrons can induce inverse Stone-Wales transition, **healing the defect graphene sheet**!
- Laser strongly enhances out-of-plane vibrations of graphene sheet (overall weakening of C-C bonds).

Mechanism of Stone-Wales defect healing

- Plot of total energy $E_{\rm tot} = E_{\rm band}(\{R_i\}) + \Phi(\{R_i\})$ (repulsive potential Φ) for absorbed energies $E_a = 0.77$ eV to $E_a = 1.32$ eV (red, has defect healing around $t = 300$ fs).

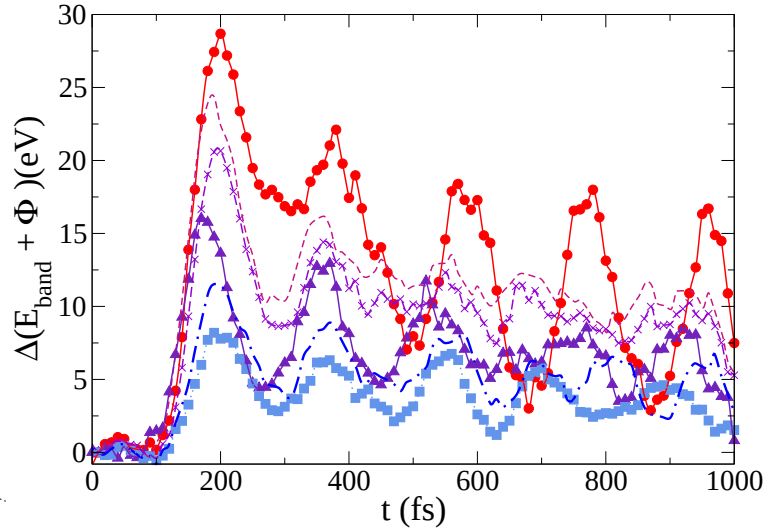

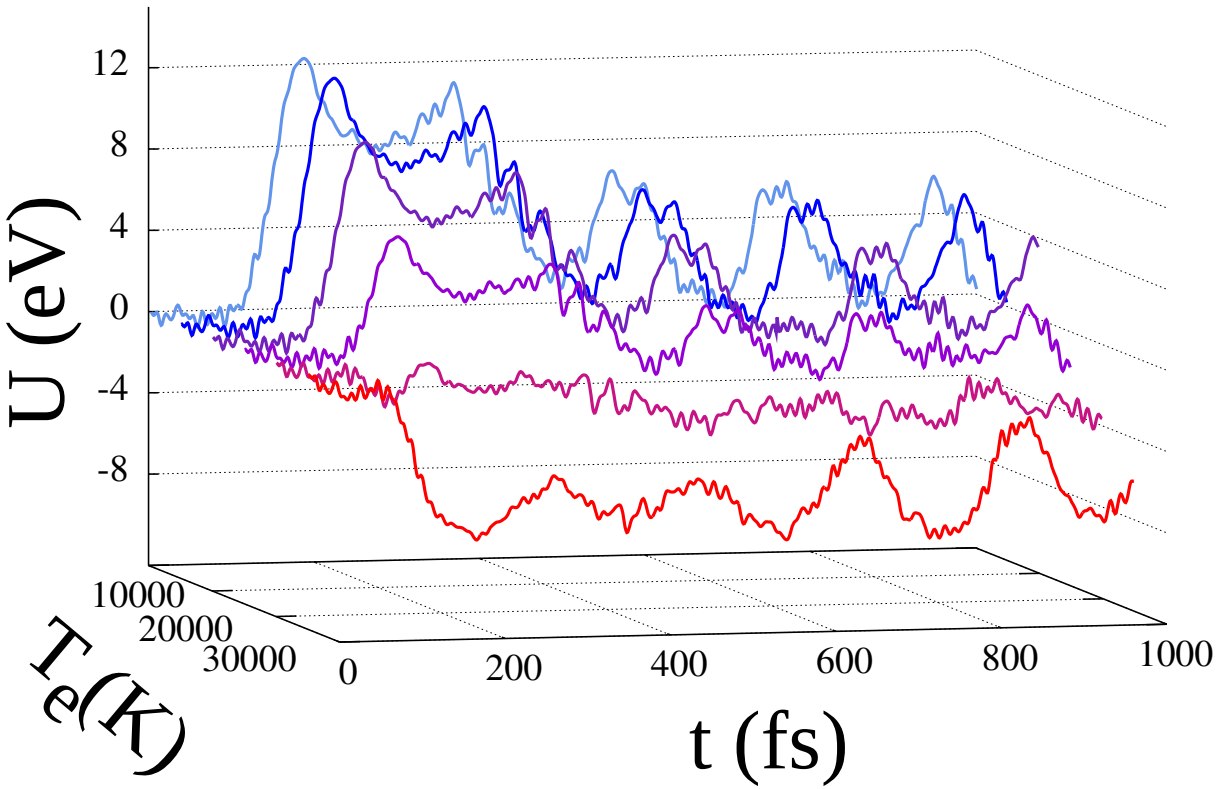

- Free energy $U = E_{\rm tot} - T_e(n_I)S_e(n_I)$ along healing trajectory for different electron temperatures: **Transition is entropy driven!**

Valencia, Romero, Jeschke, Garcia Phys. Rev. B **74**, 075409 (2006).

Laser healing of Stone-Wales defect in armchair nanotube

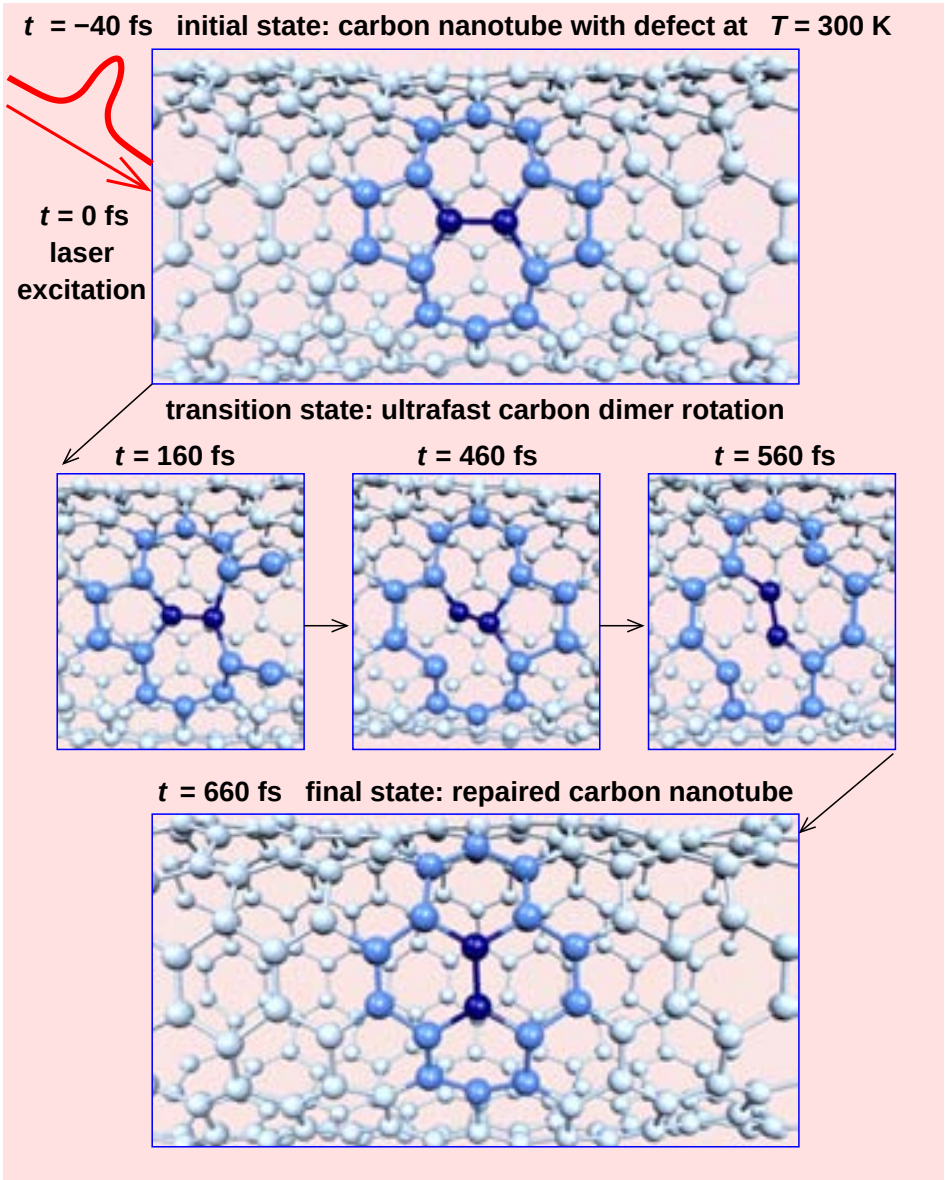

- Mechanism of defect elimination in SWNTs is the similar as in graphene sheet.
- Laser excites radial breathing mode of CNT, facilitating bond breaking in defect region.
- Important out of plane component of dimer rotation: here, dimer dives into the tube.

Romero, Garcia, Valencia, Terrones, Terrones, Jeschke,
Nano Lett. **5**, 1361 (2005).

Laser healing of Stone-Wales defect in zigzag nanotube

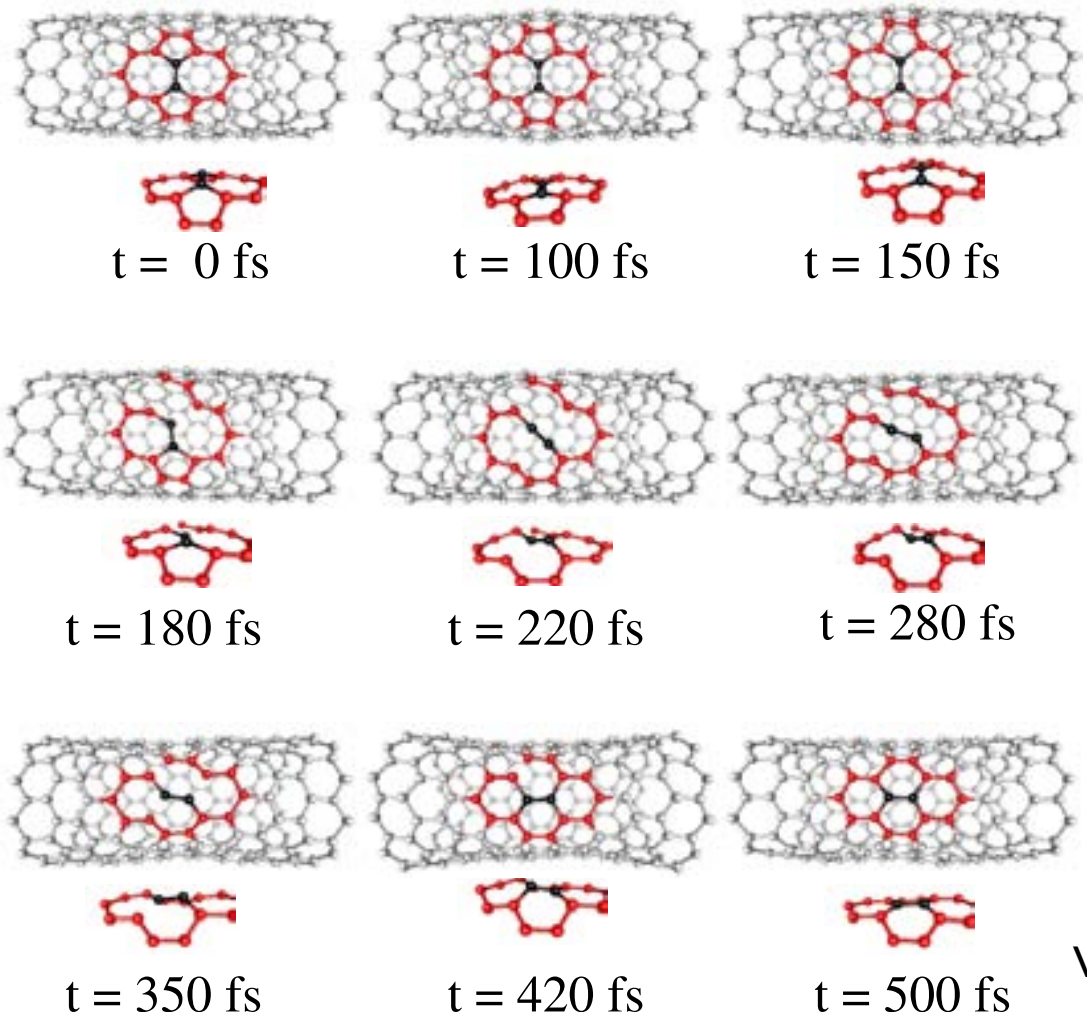

- Defect healing also observed in zigzag nanotubes. (different orientation of irregular dimer with respect to CNT axis). **General effect!**
- Possible explanation for ten times enhanced resonant Raman signal after laser irradiation: Theoretical results supply a microscopic explanation for suspected annealing effect!

Valencia, Romero, Jeschke, Garcia, Phys. Rev. B **74**, 075409 (2006).

Evolution of SWNT structure under laser irradiation

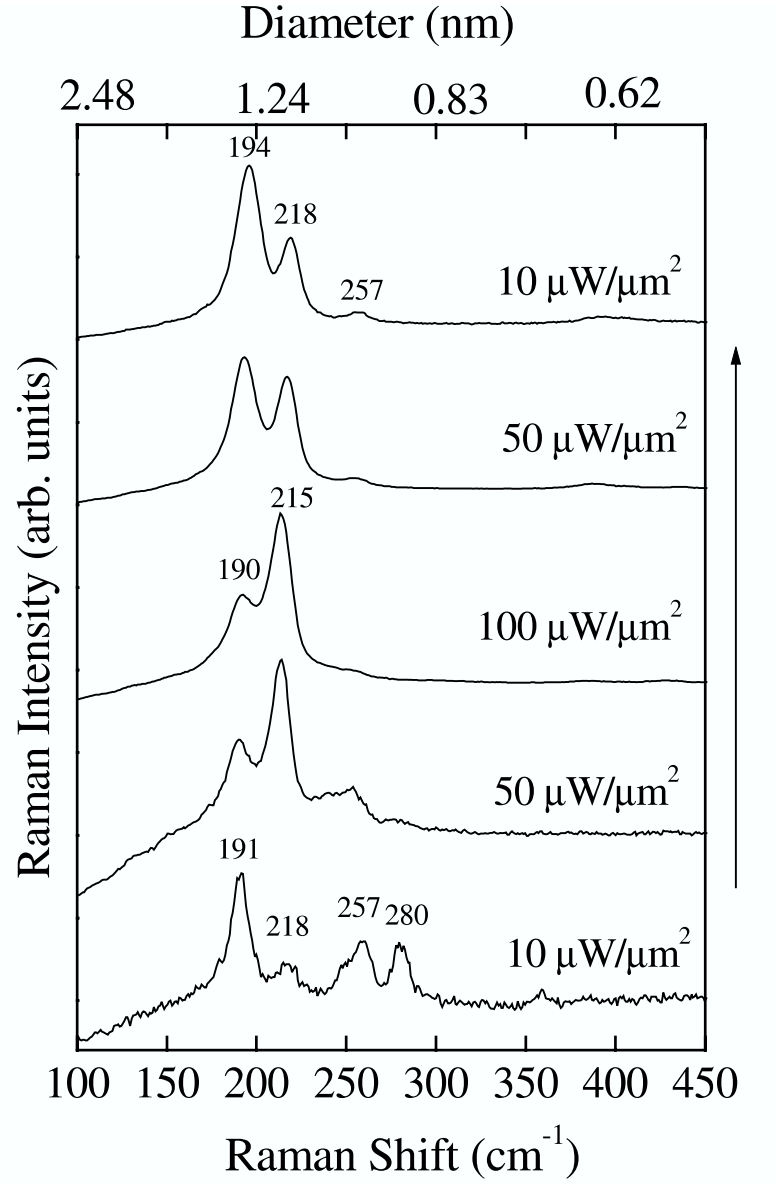

- Laser excitation of SWNT bundles at $\hbar\omega = 1.96$ eV, with intensity first increasing, then falling again.
- Observation of the radial breathing mode (RBM) frequency region. $\omega_{\mathrm{RBM}} = 248\mathrm{cm}^{-1}/d_t$, with d_t tube diameter in nm.

Corio, Santos, Pimenta, Dresselhaus, Chem. Phys. Lett. **360**, 557 (2002).

Evolution of SWNT structure under laser irradiation

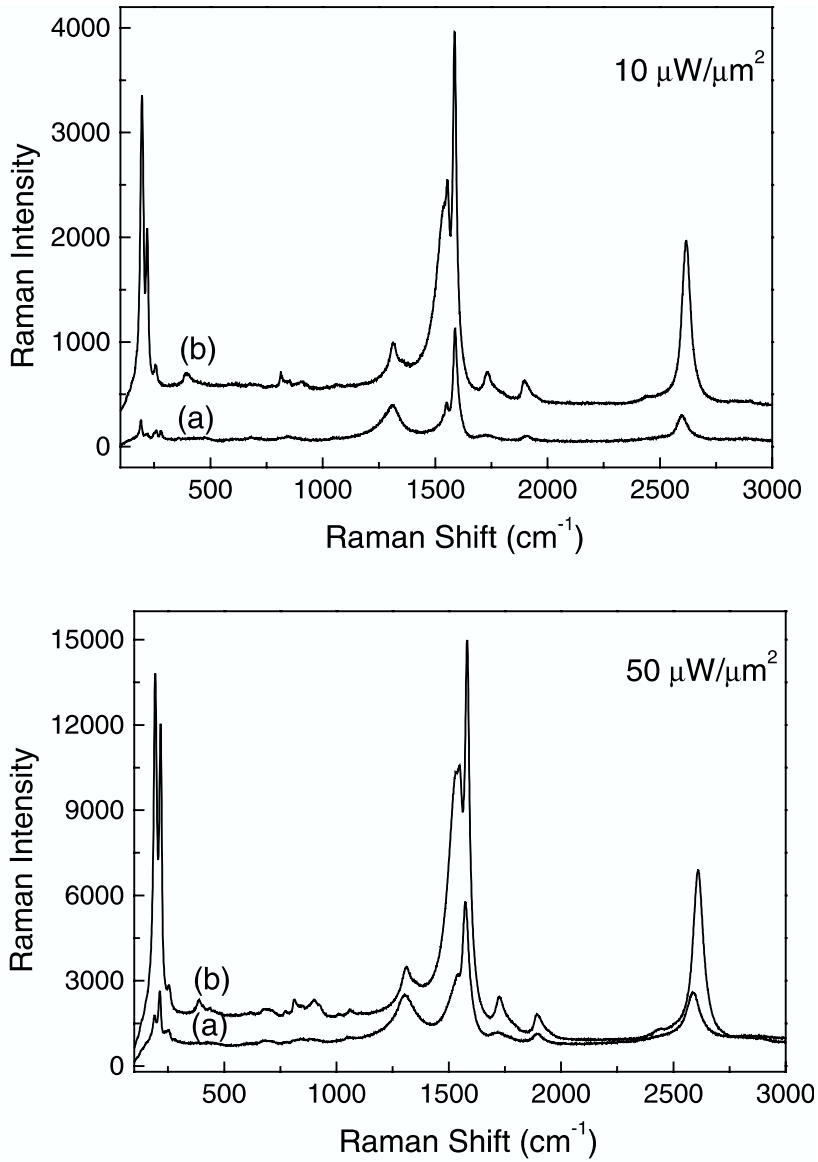

- Raman spectra before (a) and after (b) irradiation with 100 $\mu W/\mu m^2$ laser pulse; app. 10 times enhancement of intensity is observed.
- Possible explanation: Resonant Raman spectra depend strongly on sharp van Hove singularities in 1D DOS; but defects and disorder will broaden van Hove peaks. Thus, laser irradiation must have an annealing effect on SWNT bundle.

Electronic temperature and capped nanotube structure

- Color coding of structure: C-C bond length colors range from blue for $d_{C-C} < 1.4$ Å to red for $d_{C-C} > 1.52$ Å.
- Structure at constant elevated electron temperature of $T_e = 25000$ K shows significant bond expansion/weakening.
- Bond elongation, *i.e.* strain, is higher in caps.

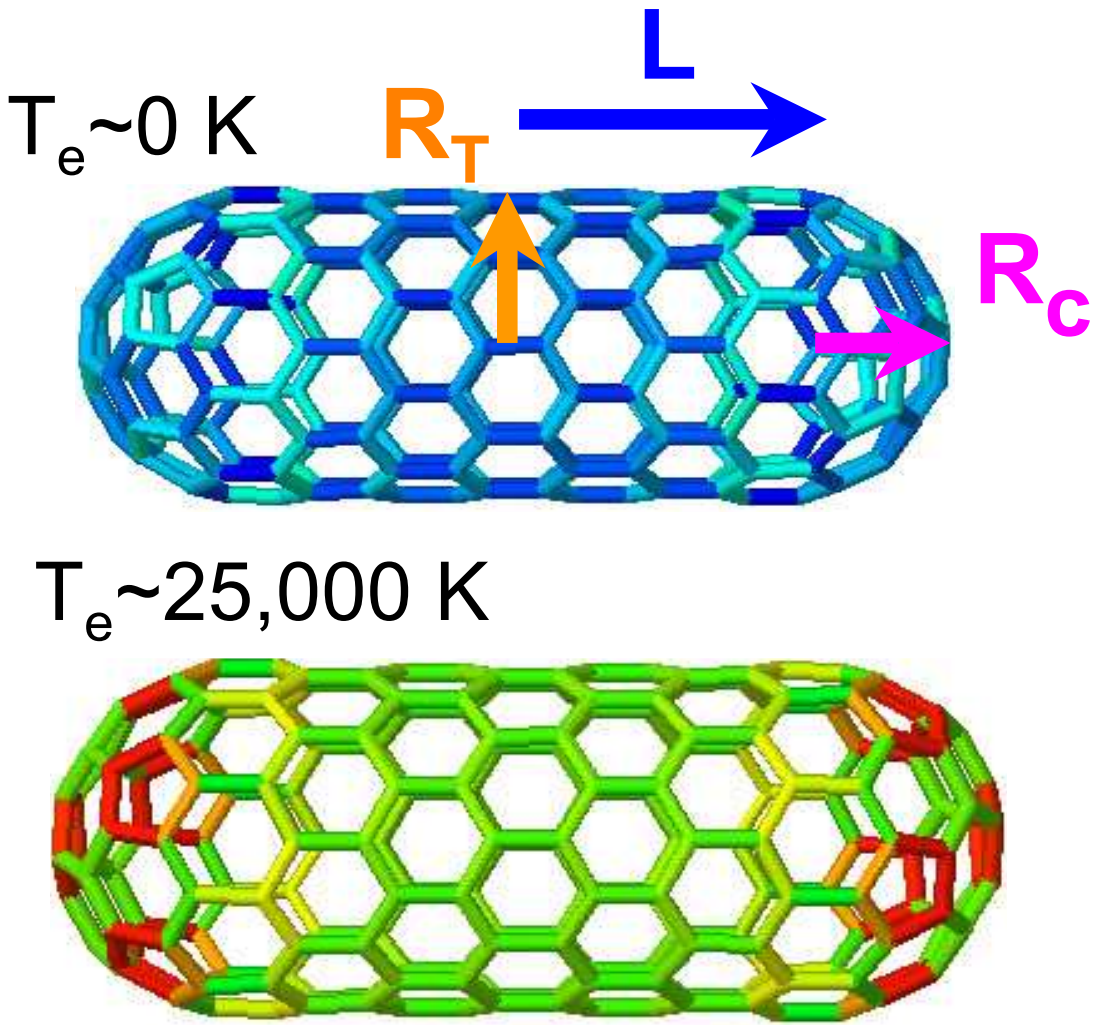

Dumitrica, Garcia, Jeschke, Yakobson, Phys. Rev. B 74, 193406 (2006).

Below threshold laser excitation of capped nanotube

- $(10, 0)$ CNT response to $\tau = 10$ fs pulse, 15% below damage threshold

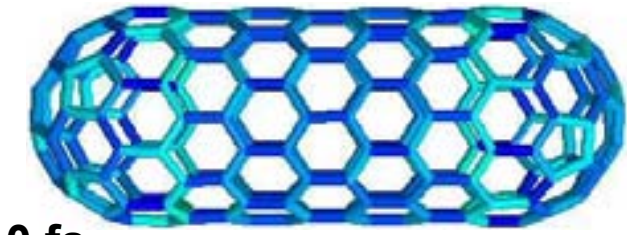

0 fs

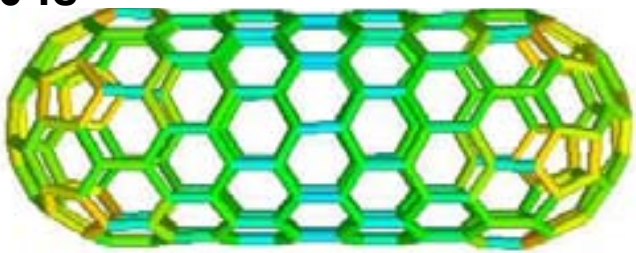

50 fs

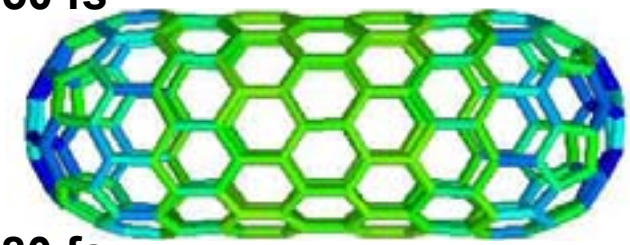

80 fs

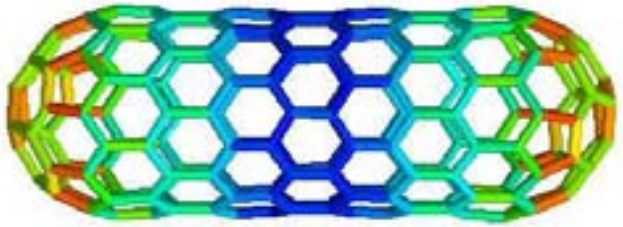

120 fs

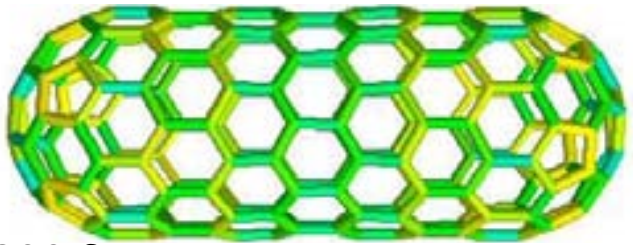

200 fs

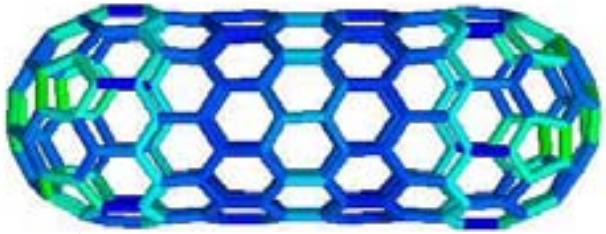

250 fs

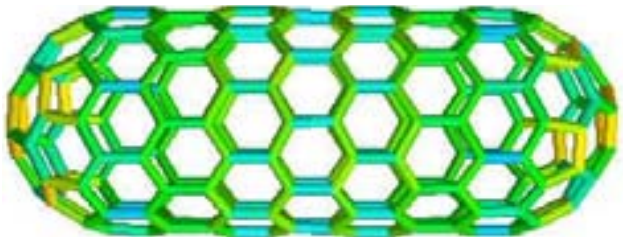

300 fs

Laser excited capped CNTs: Identification of coherent phonons

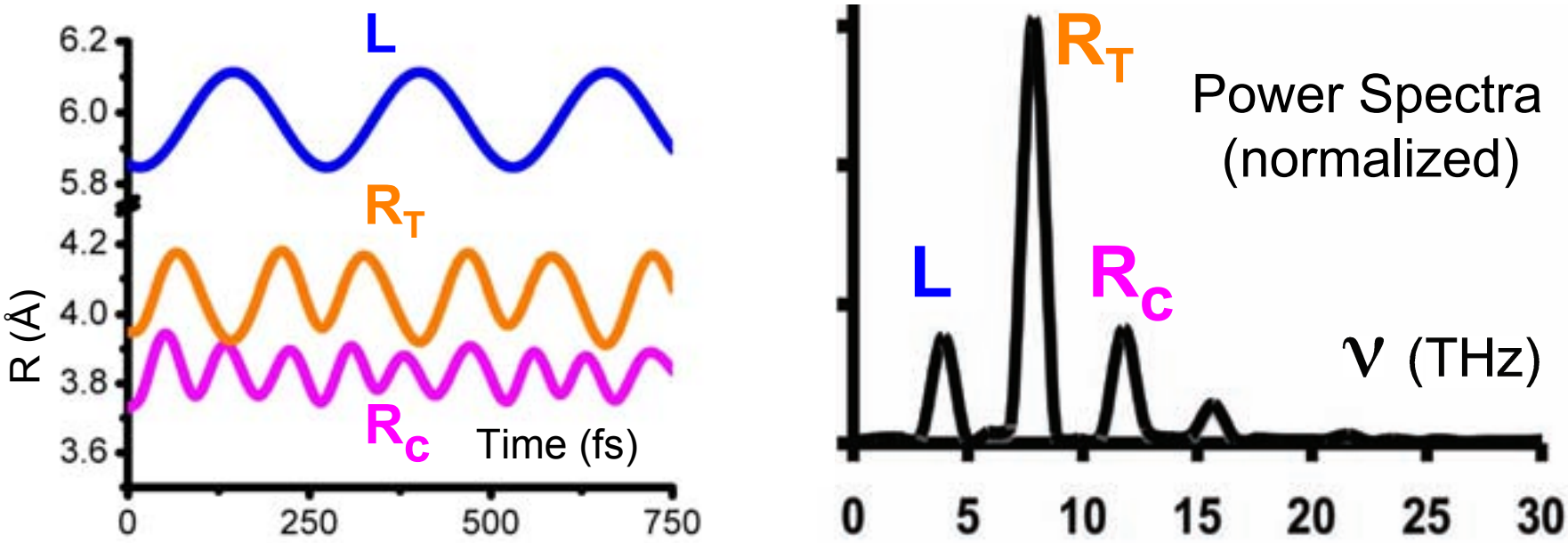

- Identification of a longitudinal breathing mode in the tube body (L), a transversal mode of the body (R_{T}) or radial breathing mode (RBM) and a breathing mode of the cap (R_{C}).
- These modes can be extracted by averaging over the coordinates (left) and by Fourier transforming the velocity autocorrelation function (right).

Laser induced cap opening: Mechanism

- Simultaneous excitation of coherent phonons with different periods.
- Strain maximum when cap and body breathing modes are of opposite phase.

⇒ **Clean separation of tube and body!**

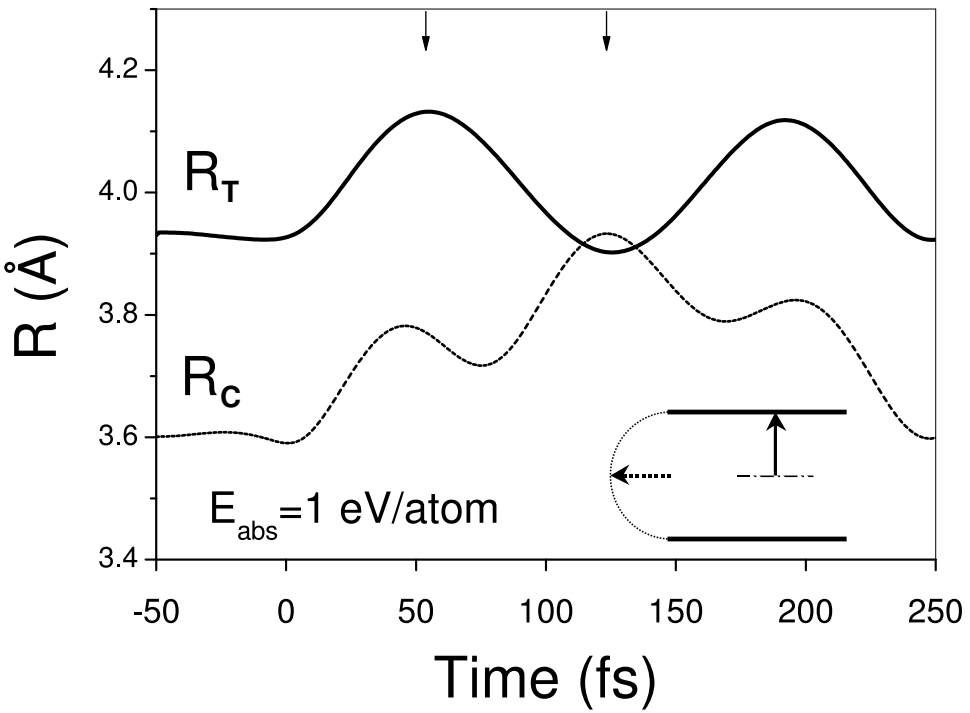

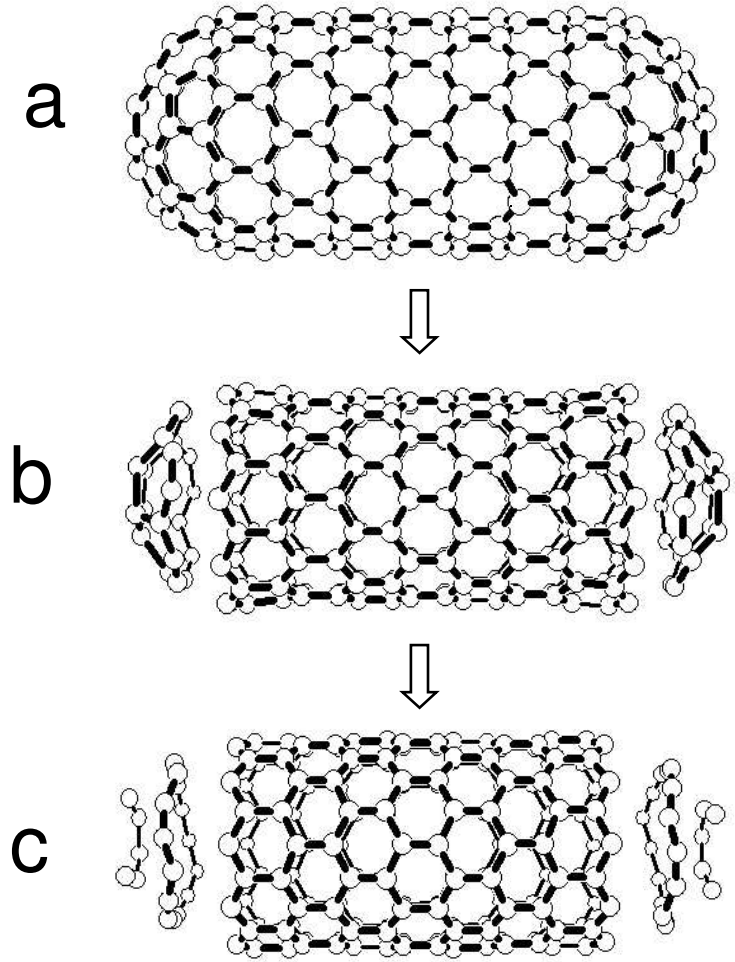

Dumitrica, Garcia, Jeschke, Yakobson, Phys. Rev. Lett. **92**, 117401 (2004).

Laser induced cap opening: Analysis

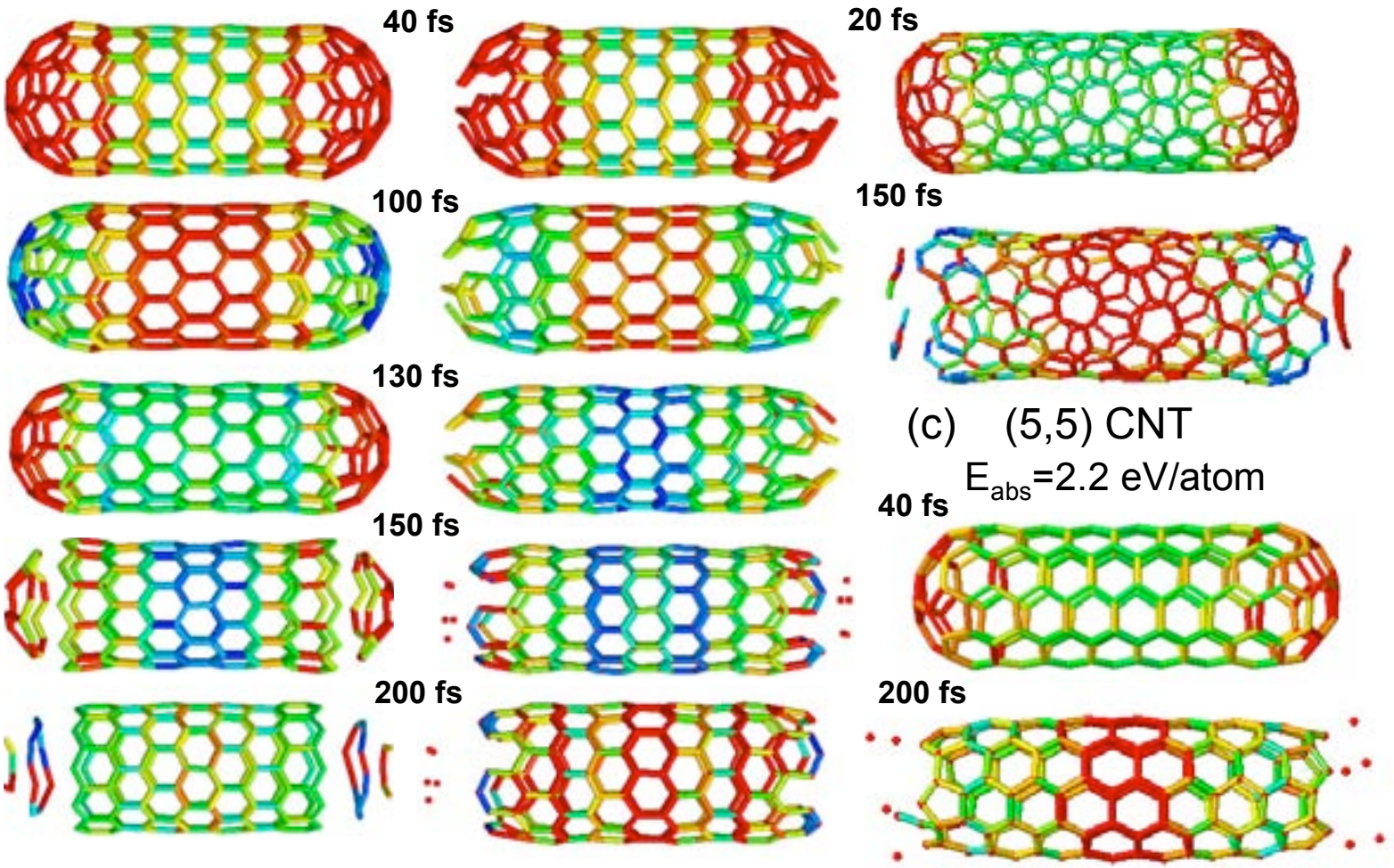

Experiment on germanium

- Ultrafast X-ray diffraction on 160 nm Ge films

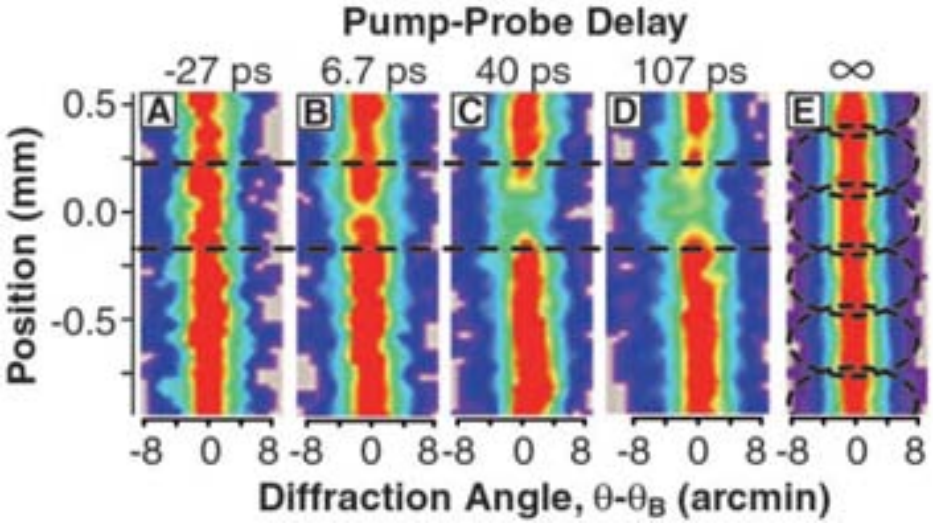

Siders, Cavalleri, Sokolowski-Tinten *et al.*, Science **186**, 1340 (1999).

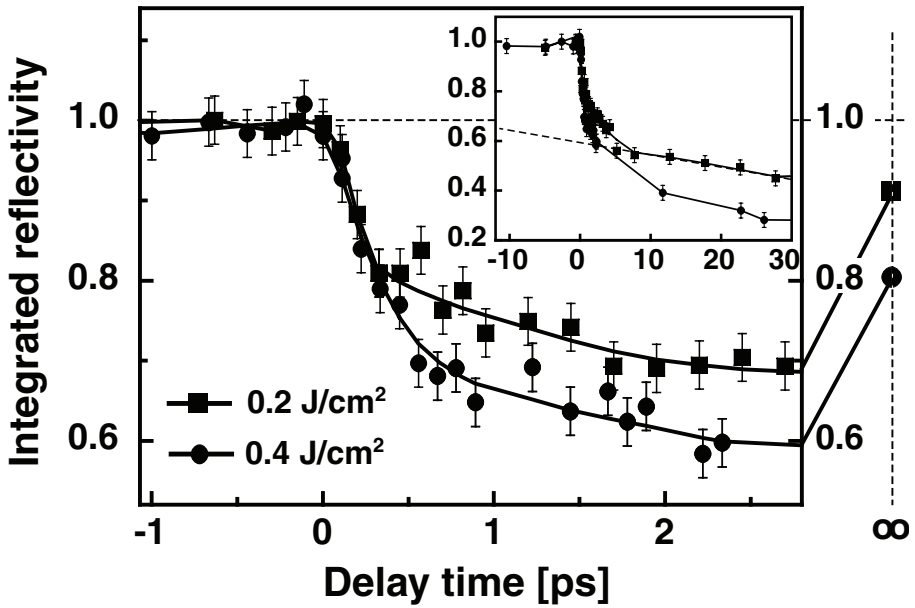

Sokolowski-Tinten *et al.*, Phys. Rev. Lett. **87**, 225701 (2001).

- 25% decrease in diffraction within 300 fs linked to ultrafast formation of 40 nm liquid film.

Coherent phonon in germanium

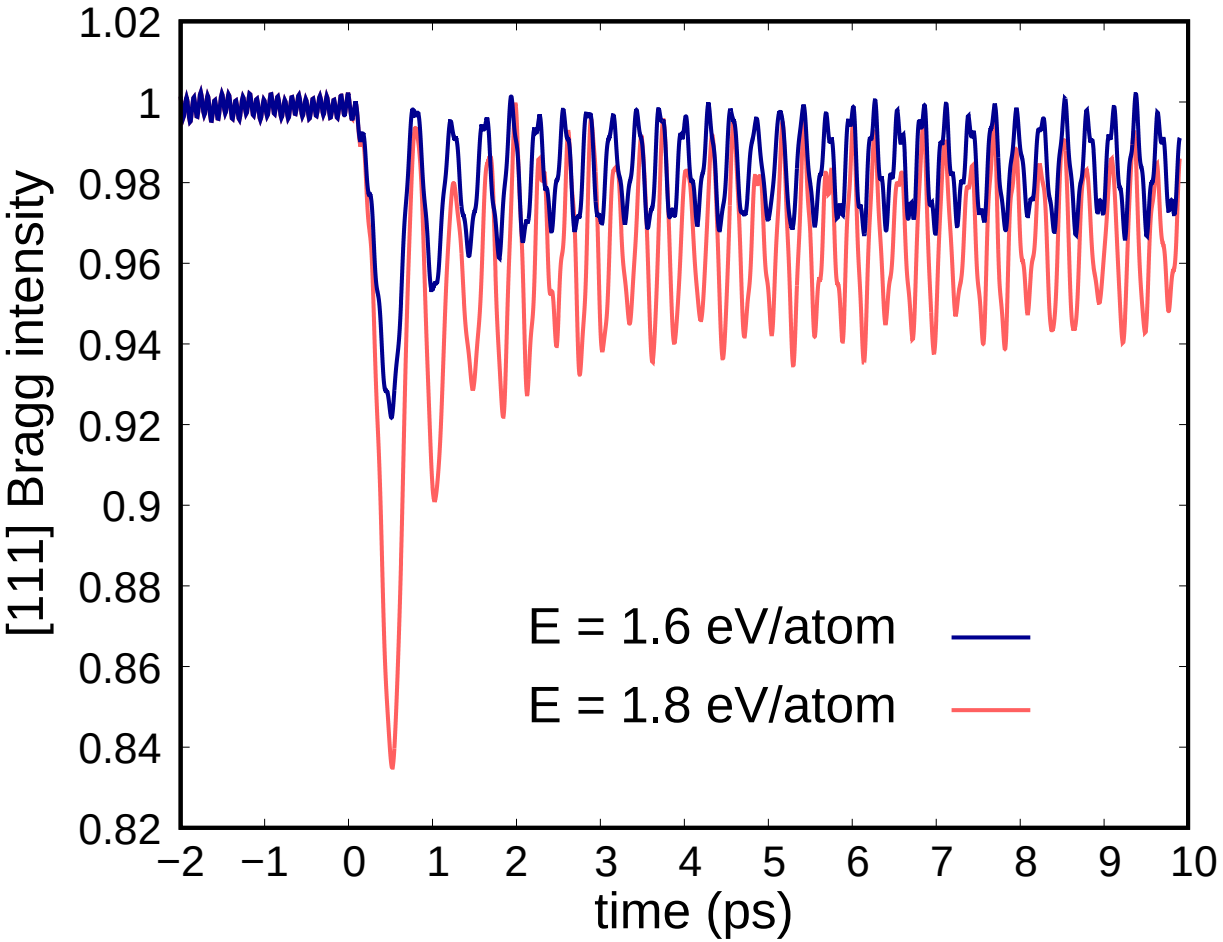

- Coherent oscillations at low laser fluences (below melting threshold $E = 2.3$ eV/atom)
- [111] Bragg peak intensity of Ge diamond bulk
- $\tau = 50$ fs pulse duration, $\tau_2 = 2.8$ ps electron-lattice equilibration
- $I_{hkl} \propto \left|S_{hkl}\right|^2$, $S_{hkl} = \frac{1}{N}\sum_l \exp\left[i\mathbf{G}_{hkl}\cdot\mathbf{R}_l(t)\right]$

Projection of motion on TA direction

- Motion along the transverse acoustic (TA) direction at the L point.
- $Q(\mathbf{k},t) = \sum_j^N e^{i\mathbf{k}\cdot\mathbf{R}_j(t)} \times \times\left[\mathbf{R}_j(t) - \mathbf{R}_j(0)\right] \cdot \mathbf{e}_\alpha(\mathbf{k})$ with $\mathbf{e}_\alpha(\mathbf{k})$ polarization vector at $\mathbf{k}$ for α =(TA,TO,LA,LO).

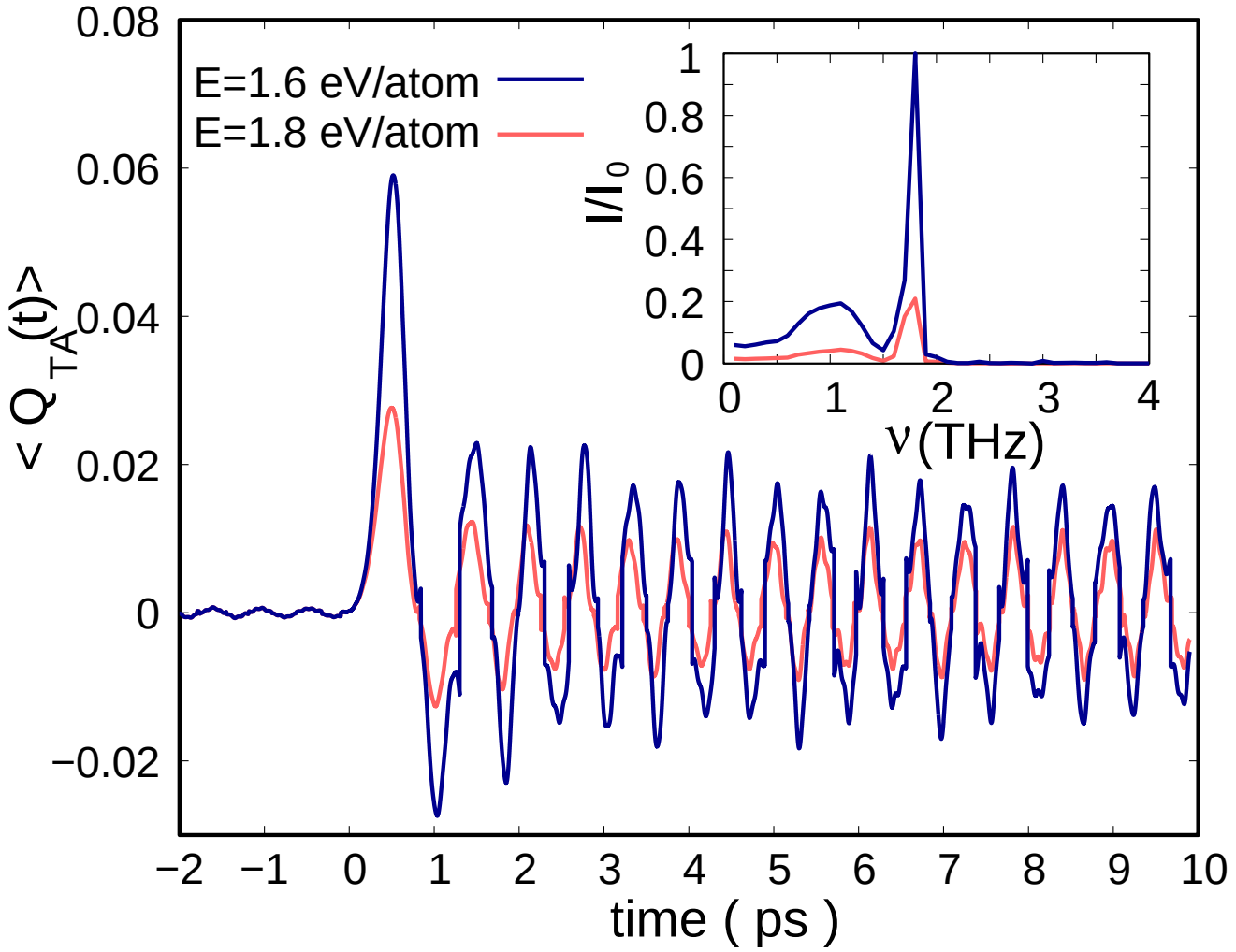

Lattice instability at higher fluence

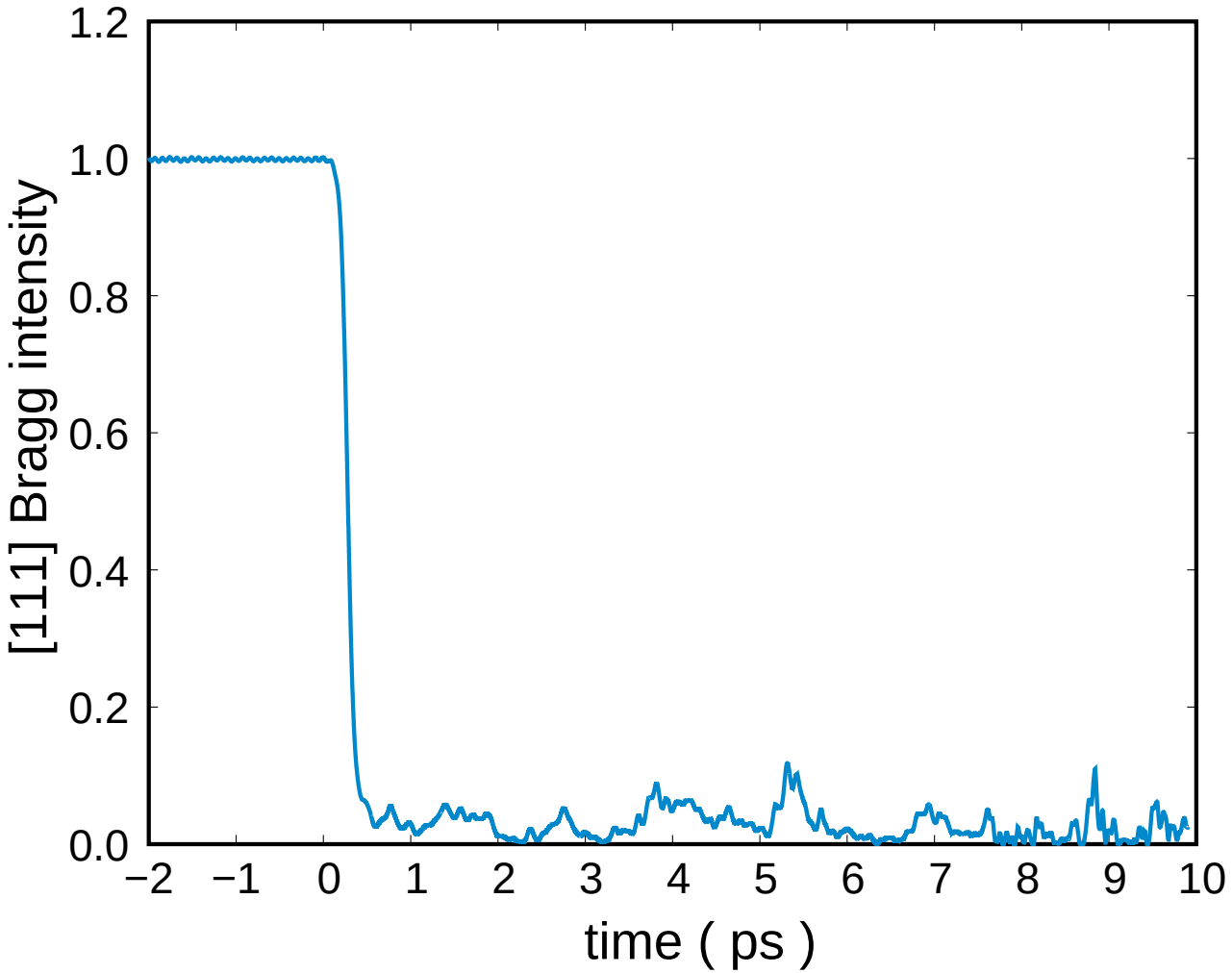

- Time dependence of [111] Bragg peak intensity for $E = 3.8$ eV/atom (above melting threshold, below ablation threshold $E = 4.2$ eV/atom).
- Bragg peak intensity disappears in < 500 ps, consistent with experiment.

Phonon softening at particular k vectors

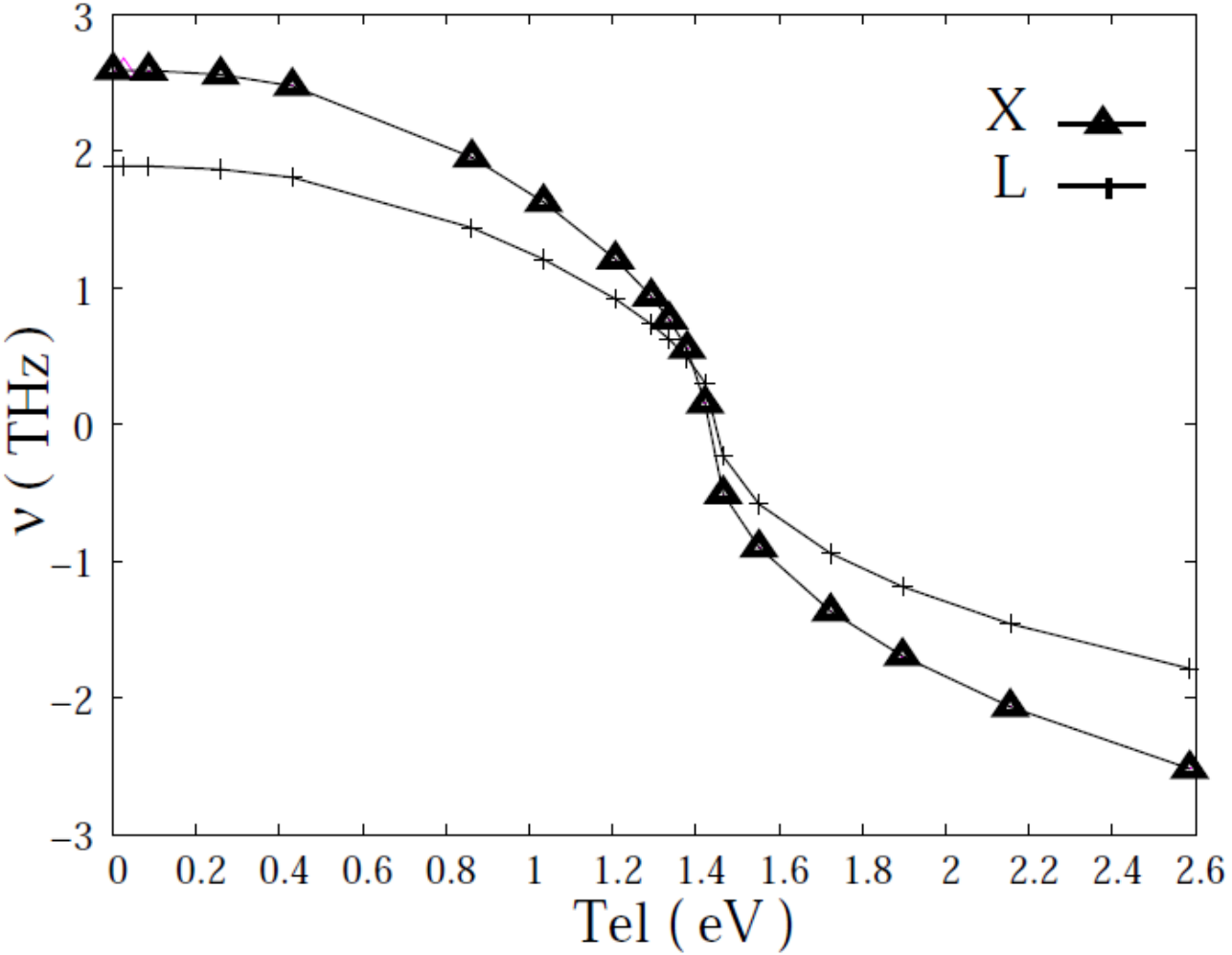

- Transverse acoustic phonon frequencies as function of electron temperature T_{el} at X and L points.
- Purely imaginary frequencies plotted as negative.

Phonon spectrum of Ge at high electron temperature

- Transverse acoustic phonons along high symmetry lines of the first Brillouin zone.
- Spectrum calculated by diagonalization of dynamical matrix, using FROPHO code.

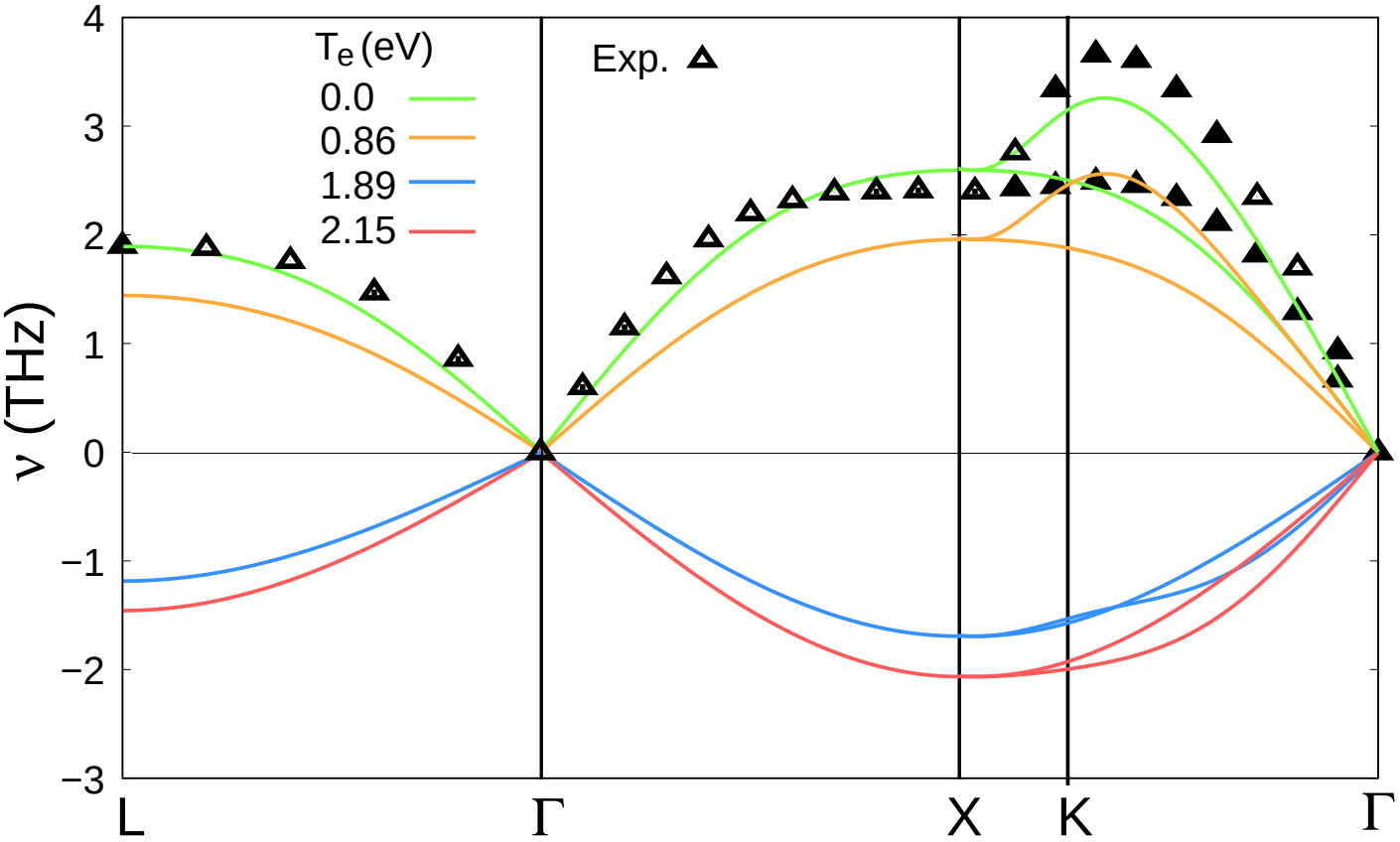

Experimental data from Phys. Rev. B **3**, 364 (1971).

Rapid phonon softening with increasing electron temperature!

Jeschke, Diakhate, Garcia, App. Phys. A **96**, 33 (2009) and Diakhate, Jeschke, Garcia, in preparation.

Outlook

- Improved treatment of electronic system:
  - calculation of matrix elements
  - more complex pulses: inclusion of polarization, chirp
  - more realistic treatment of electron-electron interactions: Solution of Boltzmann equations (together with Beata Ziaja)
- Implementation of laser pulse shapes into Car Parrinello (*ab initio*) molecular dynamics method
- Strongly correlated materials in laser induced nonequilibrium?

Conclusions

- Tight binding based molecular dynamics on time dependent potential energy surfaces successfully describes microscopic structural changes following femtosecond laser excitation of materials.
- Diamond: Ultrafast laser induced graphitization
- Graphite: Prediction of low intensity ablation mechanism; confirmed by experiment.
- Silicon: Formation of large clusters.
- Capped nanotubes: Laser excitation of coherent phonons allows precise structural modification. Possibly more generally useful?
- CNTs with defects: Laser pulse induces entropy driven defect elimination. Laser induced nonequilibrium represents fascinating way to manipulate nanostructures.
- Softening of phonons in Germanium.